Climate induced Congestion in Ports: General Equilibrium Consequences on Transportation and Trade

Jeanne Astier*

March 2026

Preliminary and Incomplete.
Please do not circulate.

Abstract

This paper studies the impact of climate change on ports and its consequences for maritime transportation and international trade. Rising sea levels and associated weather events threaten port operations in a spatially heterogeneous way. Because container shipping operates as a global network, local disruptions propagate and create spillovers that affect even ports not directly exposed. I combine high-frequency satellite shipping data with marine weather observations to estimate how adverse water-level conditions reduce port efficiency and raise transportation costs. I embed these estimates in a quantitative trade model with a shipping network and endogenous port congestion. Economies of scale on shipping links rationalize the sparse network structure and allow its topology to respond endogenously to climate shocks in counterfactual exercises. Using IPCC projections under the SSP5-8.5 scenario, I find that by 2100, ports will experience water-level increases of up to 1.3 meters, translating into welfare losses of up to 1.1% of real output. These losses reflect both a direct effect from a port's own exposure to rising water levels, and an indirect effect from spillovers propagating through the shipping network from other affected ports. As a result, even ports facing no local increase in water levels suffer welfare losses. This underscores the global reach of climate-induced disruptions to maritime infrastructure.

Keywords: shipping, climate change, trade, weather, transportation, sea level rise

*Center for Research in Economics and Statistics (CREST), Institut Polytechnique de Paris. Email: jeanne.astier@ensae.fr.

This paper benefited from comments by Geoffrey Barrows, Johannes Boehm, Thibault Fally, Simon Fuchs, Cécile Gaubert, Florian Grosset-Touba.

1 Introduction

The impact of climate change on economic outcomes has been widely documented, in particular for weather events happening on land through the channels of agriculture, productivity, capital. The role of trade in mitigating climate change impact is also extensively studied by the environmental economics literature (Costinot et al., 2016; Gouel & Laborde, 2021; Carleton et al., 2023). However, the sensitivity of trade itself to climate change seems overlooked: trade costs might be impacted by climate change. This could happen through the transportation channel, which can be impacted by weather conditions both on land and at sea. Looking at the effect of climate change on trade costs allows to uncover a new part of the climate damage function, and to provide new elements on the debate of trade as a mitigation factor.

In this paper, I am focusing on the impact that climate change might have on trade costs through the channel of sea level rise affecting on ports infrastructure and maritime transportation. International trade is heavily relying on maritime freight: about 80% of traded goods are seaborne (UNCTAD, 2023). Yet, the shipping sector is already often disrupted by weather events, especially those affecting port infrastructures.[1] Climate change is expected to worsen the weather conditions affecting ports, through sea-level rise and associated weather events (wind, waves, storm surge, coastal flooding...) (Pörtner et al., 2019). Such adverse weather translates into non-operability days for the ports, during which their activity is stopped or significantly reduced (Izaguirre et al., 2021). Their reduced capacity to receive ships might in turn cause congestion, resulting in increases of transportation costs (Brancaccio et al., 2024). Given the network structure of shipping (Heiland et al., 2019; Brancaccio et al., 2020; Ganapati et al., 2021), the effect of these local weather shocks propagate to other ports and shipping routes, triggering a ripple effect with global consequences.

This paper studies the global impact of climate change effects on ports and its consequences on international trade, in the context of the container-shipping network. I leverage detailed shipping and weather data to estimate how weather shocks affect ports efficiency, and hence raise transportation costs. I then include this effect in a model of international trade with a shipping network, featuring endogenous port congestion, based on Allen & Arkolakis (2022). I further endogenize the network structure through economies of scale on shipping links. This model is then used to estimate counterfactuals with sea level rise projections: I can quantify the global effects on transportation and trade given the spillover mechanisms at play, as well as the spatial distribution of the heterogeneous local effects.

I rely on satellite automatic identification system (AIS) technology, a novel source of data

[1] See for instance the closure of New York and New Jersey ports in October 2012 because of Hurricane Sandy, more recently the closure of Florida ports during hurricane Milton in October 2024.

increasingly used in the trade literature (Heiland et al., 2019; Brancaccio et al., 2020; Ganapati et al., 2021). I observe the exhaustive universe of port calls made by containerships in about 1,700 ports between 2015 and 2023, with their exact hour and date. These data allow to measure port dwell time (i.e. the time spent by ships in the port to be unloaded and reloaded), an indicator of port efficiency (Brancaccio et al., 2020). I combine this measure with weather data at the location of the ports, in particular water level daily averages from the global reanalysis ERA-5 dataset (Hersbach et al., 2023). Reduced-form evidence shows that higher water levels significantly affect port efficiency: a +1m increase in average water level over a quarter (equal to around 1.25 standard deviations) increases average dwell time over that quarter by approximately 12.2%. I find that this effect is non-linear and mostly driven by days with extreme water levels. Reduced-form exercises are also informative about adaptation mechanisms at play. A heterogeneity analysis suggests that ports exposed to higher water level on average over the 2015-23 period, are less sensitive to a day with high water level than ports facing lower average levels. This evidence of heterogeneity is consistent with adaptation of port infrastructure to rising sea levels.[2] I also find evidence that the shipping flows are adapting high water levels in ports. In particular, I observe traffic diversion away from the most affected ports: as some ports become costlier to transit due to elevated water levels, shippers gradually reroute cargo to avoid them.

The IPCC (Pörtner et al., 2019) projects substantial water level rise in the coming decades. Quantifying the long-run effects of this shift requires accounting for the adaptation mechanisms highlighted by the reduced-form evidence. To do so, I rely on a spatial economic model with optimal shipping route choice and endogenous traffic costs. I adapt the workhorse model of Allen & Arkolakis (2022), often used to study transportation between cities (e.g. Fuchs & Wong 2024), to an international trade and shipping setting. I consider that firms can export the goods they produce through ports, that are connected by a shipping network. To export from an origin to a destination, firms choose an optimal route that can go through several intermediate ports.[3] As opposed to the road network considered by Allen & Arkolakis (2022), I model congestion not on the *links* of the network but on the *nodes* – i.e. the ports: the cost of going through a port depends on the congestion in this port. Indeed, Brancaccio et al. (2024) show that a greater number of ships in a port forces ships to queue and hence increases the ships dwell time and service cost. I further assume that congestion in a port depends not only on the traffic it faces but also on the availability of its infrastructures, that can be affected by weather shocks. I also endogenize the network structure itself through economies of scale on link costs. The shipping network is sparse: not all pairs of ports are directly connected, and establishing a new bilateral link requires no infrastructure investment, making the topology more flexible than terrestrial

[2] Christodoulou et al. (2019) give anecdotal evidence of ports infrastructure investments making them more resilient to adverse weather conditions, such as sea walls.

[3] Ganapati et al. (2021) highlight that most of shipping transportation is indirect, the goods stopping in several intermediate ports between the origin and destination ports.

transport networks. I rationalize this sparse structure through economies of scale on shipping links: when traffic on a link is insufficient to amortize its fixed operating costs, the link becomes prohibitively expensive and effectively inactive in equilibrium. This allows the network topology to respond endogenously to climate shocks, so that the set of active shipping links adjusts in counterfactual exercises. Using exact hat algebra techniques, I can then solve the model to determine the welfare effects of a counterfactual weather.

To quantify counterfactual scenarios, I need to estimate two key parameters: the elasticities of ships' dwell time to port congestion and to weather shocks. I leverage detailed AIS shipping data to estimate those, relying on a specification derived from the model – similarly to Fuchs & Wong (2024) but with an additional weather effect. The estimates I obtain show that a 1% increase in port traffic raises ships dwell time by 0.22%, while +1m water level increases the dwell time by 4.3% – this effect being reduced by 0.7 percentage point when the port is subject to +1m higher long-run average water level (adaptation). These effects are significant at the 5% level with a strong first stage.

Using these estimates and taking other structural parameters' values from the literature, I run a fixed point algorithm to solve for counterfactuals. I rely on country-level population and economic outcome from the World Penn Tables, and allocate those to ports by creating port catchment areas. I use IPCC's sea level rise projections (Garner et al., 2022) to compute the change in water level for each port: there is significant heterogeneity, with some ports facing little to no increase in water level while other will experience more than +1m by 2100 (according to scenario SSP5-8.5). The model predicts a significant welfare loss, up to −1.1% of real outcome for the most affected ports (in the South-East Asia, East Coast of the USA).

The counterfactual exercise results show that a port's welfare loss is correlated with its own rise in water level, but not perfectly. Indeed, even the ports facing no change in water level will suffer a decrease of real outcome. This result highlights the importance of indirect effects coming from other ports through the shipping network. These results are obtained with a fixed network structure; allowing the network to adjust endogenously through economies of scale on link costs is work in progress. It would further amplify these reallocation effects, as shipping companies reroute traffic away from the most climate-affected ports.

This project builds on the trade literature including transportation networks. While this literature originally considers land transportation infrastructures at the country level, like highways or railroads (Fajgelbaum & Schaal, 2020; Allen & Arkolakis, 2022; Fuchs & Wong, 2024), an increasing body of works adapts these tools to study maritime transportation (Heiland et al., 2019; Brancaccio et al., 2020; Ganapati et al., 2021; Ludwig, 2024). I contribute to this literature

in several ways. First, I displace congestion from the *links* of the network to the *nodes*, based on the framework of Allen & Arkolakis (2022) and similarly to Fuchs & Wong (2024), to better represent port-level bottlenecks in shipping. Second, I endogenize the network structure itself through economies of scale on link costs: rather than taking the set of active shipping links as given, I rationalize the sparse topology observed in the data through a mechanism whereby links with insufficient traffic become prohibitively expensive and effectively inactive in equilibrium, allowing the network to adjust endogenously to climate shocks. Ganapati et al. (2021) estimate economies of scale at the leg level in container shipping and show that they underpin the hub-and-spoke structure of the global trade network, but take the network topology as given; I build on this insight to endogenize the network structure itself. Third, I study transportation in an international context rather than between cities of the same country, adapting the workhorse model of Allen & Arkolakis (2014) to include labor immobility and trade deficits. While other papers in an international context aggregate ports to the country level (Ganapati et al., 2021; Ludwig, 2024)[4], I provide a mapping between countries and ports by building port catchment areas.

I also relate to the growing literature studying shipping with satellite AIS data. Most of this literature focuses on ships trips in a trade context (Heiland et al., 2019; Brancaccio et al., 2020; Ganapati et al., 2021), while a recent paper by Brancaccio et al. (2024) uses these data to study ports at the micro, country level. I try to connect these two approaches by including port congestion mechanisms identified by Brancaccio et al. (2024) in a global trade setting. The closest paper related to my work is Fuchs & Wong (2024), which studies a multi-modal transportation network including, among others, nodes congestion, also estimated using AIS data. My contribution with regard to this paper is to go from a country-level approach to a global setting and to propose a different application, to climate change effects quantification. I also propose to study a new mechanism which, to the best of my knowledge, has not been studied yet in this trade and shipping literature: the effect of weather shocks.

This weather shocks mechanism relates the paper to the environmental literature, first on the strand trying to quantifying the effect of climate change on economic outcomes. This impact has been widely documented for weather events happening on land – such as temperature shocks (Dell et al., 2012), hurricanes (Deryugina et al., 2018), floodings (Balboni et al., 2023), wildfires (Wang et al., 2021) ... – through channels like agriculture, productivity, capital. I propose to study sea weather shocks, focusing on water level, and to uncover a new channel, the transportation sector. While some environmental works have been investigating the link between transportation and climate change, they mostly focus on how transportation contributes to climate change through emissions (see for instance Ludwig 2024 for the shipping sector). My perspective is rather to study how climate change related weather events can impact the transportation sector.

[4]Which results in disregarding land-locked countries.

Finally, I also build on works studying in a reduced-form way the local impact of weather shocks on port operations (Becker et al., 2018; Christodoulou et al., 2019). I try to include these local effects in a global shipping framework, to include spillovers and quantify a global impact on economic outcome. I rely on the work of climate scientists Izaguirre et al. (2021) which provide evidence of the sea weather shocks affecting port operations and document the spatially heterogeneous effects that climate change will have on ports.

The rest of the paper is organized as follows. Section 2 gives some elements of context about container-shipping. Section 3 presents the data used and provides reduced-form evidence of the effect of weather shocks on port efficiency. Section 4 details the economic geography model with shipping. I estimate the key parameters of this model in section 5. Section 6 presents the counterfactual exercises and their results.

2 Context about Container-Shipping

Containerships carry essentially manufactured goods. As explained by Brancaccio et al. (2020), they operate like a public bus system, with a pre-specified set of ports (called a *service*) at which a ship stops successively. At each port, containers can enter or leave the ship. They can also change ship (trans-shipment). Figure 1 shows an example of containership service between Europe and America, going through the ports of Charleston - Miami - Veracruz - Altamira - Bayport - New Orleans - Le Havre - Antwerp - Rotterdam - Bremerhaven.

The set of services constitutes the containership *network structure*: this is the set of all the direct links between two ports that exist, i.e. the set of links over which containers can flow. This network is sparse: not all pairs of ports are directly connected. As a consequence, containers traveling from an origin to a destination might go through several intermediate ports, just because these ports are part of the ship service. For instance, in the service depicted in Figure 1, if a firm wants to export a container from New Orleans to Rotterdam, it would be stopping at Le Havre and Antwerp in between. In this sense, most of container-shipping is indirect (Ganapati et al., 2021). This is quite different from bulk carriers for instance, that would go directly from origin to destination without intermediate stops – operating like a taxi, rather than a bus. This indirect structure of shipping creates a potential for spillover effects: a port being down will not only affect the goods having this port as an origin or a destination, but also all the goods flowing through this port as an intermediate stop. For instance in Figure 1, containers going from New Orleans to Rotterdam would be impact by a disruption at Antwerp.

In the work presented below, I consider the network structure as fixed for the counterfactual

Figure 1: Example of a containership service between America and Europe

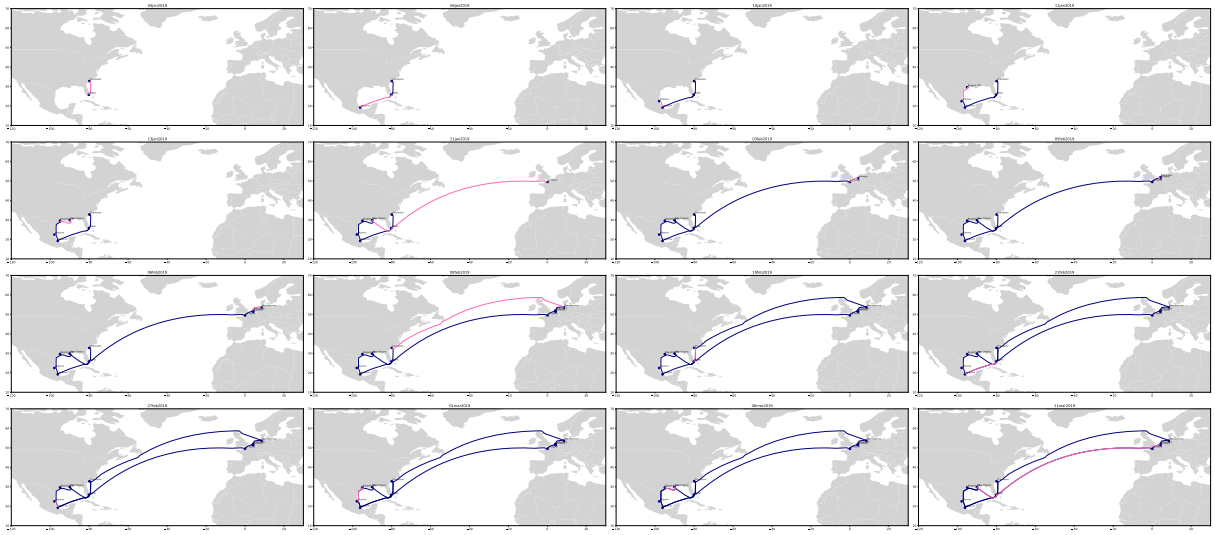

Note: these maps represent the trajectory of a containership from January to March 2019. Each pink line depicts the journey of the ship made on the day shown at the top of each map; the dark blue lines depict the journeys made by the ship in the previous days. The first row first column map shows the first trip of the ship from Charleston to Miami on January 4th; the first row second column map shows the next trip from Miami to Veracruz on January 6th; then from Veracruz to Altamira, etc. On Februry 8th (third row second column), the ship ends its service by going back to Charleston. It then starts another round, going through the same ports.

exercises and study how traffic flows reallocate within this structure. However, as discussed in Section 4, the sparse topology of the network can be rationalized through economies of scale on link costs, which would allow the network structure to respond endogenously to climate shocks.

3 Data and Reduced-Form Evidence

3.1 Shipping and Weather Data

AIS shipping data I use shipping data based on satellite automatic identification system (AIS) technology, provided by Alphaliner. The dataset covers all containerships and their detailed port calls (i.e. anytime they enter or leave a port, with the exact position and time) between 2015 and 2023. I observe a large set of ports (around 1,700) all around the world, with varying traffic intensity, as the Figure 2 shows.

I can use AIS shipping data to build a measure of port efficiency (Brancaccio et al., 2024): the port dwell time, measuring how long ships spend in the port (computed as their time of departure − time of arrival). It describes the time required by the port to unload and reload the ships, and hence measures the efficiency of port operations. Averaging the dwell time of all ships[5]

[5]Dwell times are weighted by the ships capacity, as bigger ships take longer to unload and reload.

Figure 2: Ports observed in the shipping data, by traffic intensity (2015-2023)

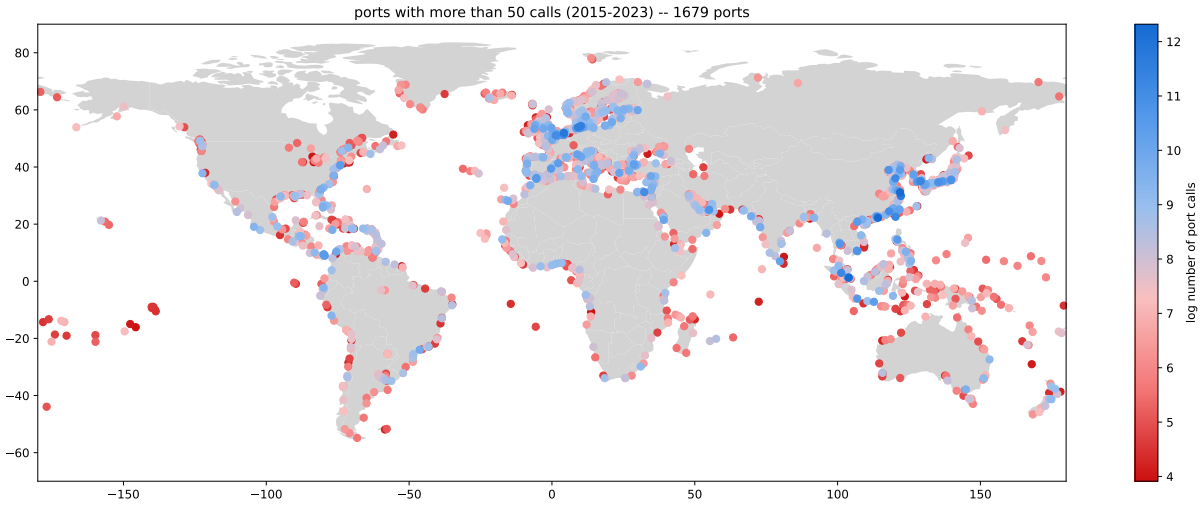

Note: The traffic intensity is computed as the logarithm of number of entering port calls over the total period.

going through a port over a period yields an aggregate measure of the port's efficiency over this period. Figure 3 depicts the monthly dwell time for the top 400 ports (in terms of traffic over the 2015-2023 period)[6] on the left panel, and for one specific port (the port of Miami, Florida) on the right panel. It highlights the significant volatility in port efficiency.

Sea weather data Port efficiency can be affected by various weather factors (Izaguirre et al., 2021): wave height, water level, wind speed, total precipitation, storm surge... I focus on total water level, as this factor will be the most important with climate change and sea level rise (Pörtner et al., 2019). I collect daily values of total water level (in deviation from 1986-2005 average) from the global reanalysis ERA-5 dataset (Hersbach et al., 2023). I combine these gridded data at the 0.25°x 0.25° level with ports geographical positions, to get daily observations of port weather. Figure 4 plots the monthly average water level over the period for the top 400 ports on the left panel, and for one specific port (the port of Miami, Florida) on the right panel. There is a clear seasonality pattern, with higher water levels around July and lower ones around December. There is also an increasing trend over the period.

[6]These ports will be the ones considered for counterfactuals later on.

Figure 3: Monthly average port dwell time, computed from AIS containership port calls (2015-2023)

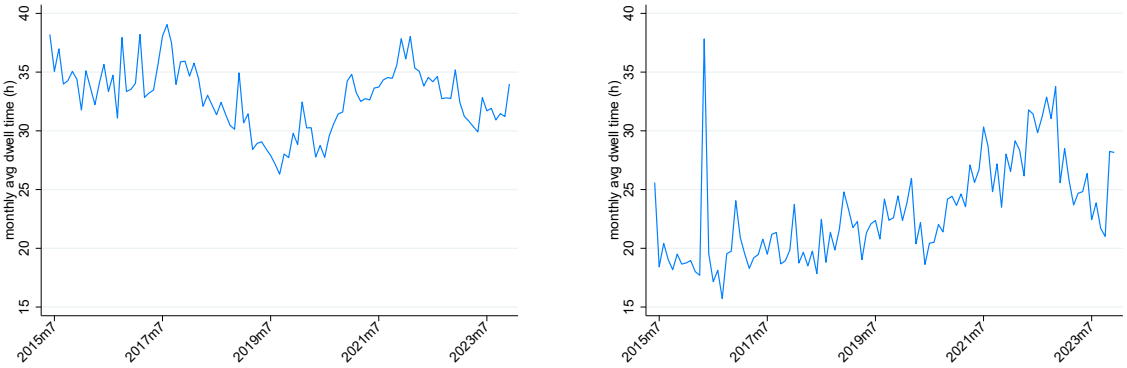

(a) Average over top 400 ports

(b) Port of Miami, Florida (US)

Figure 4: Monthly average port total water level, computed from ERA-5 reanalysis data (2015-2023)

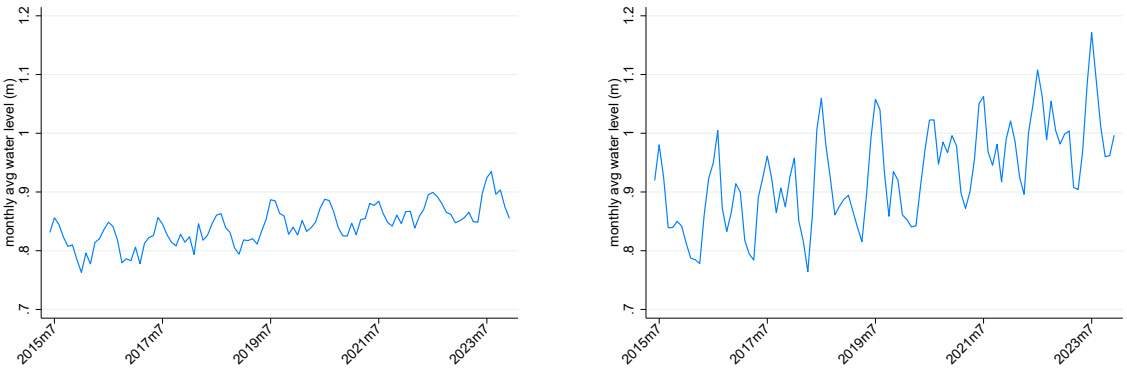

(a) Average over top 400 ports

(b) Port of Miami, Florida (US)

3.2 Reduced-Form Evidence: Effect of Weather Shocks on Port Efficiency

I combine shipping data with water level observations, to produce evidence of weather impact on port efficiency. I first provide evidence of the direct effect of a port's weather shocks on its efficiency, then highlight potential mechanisms triggered by these effects in the shipping network.

3.2.1 Direct effect of local shocks

I test the effect of a port's weather on its efficiency with the following specification:

$$\ln(\text{time})_{it} = \alpha + \beta \ \text{waterlevel}_{it} + \delta_i + \delta_t + \epsilon_{it} \tag{1}$$

where time_{it} measures the average dwell time in port i over period t, waterlevel_{it} is the average total water level at port i during period t, δ_i is a port fixed-effect, and δ_t a period fixed effect. Standard errors are clustered at the port level. I consider several periods t: day, week, month, quarter. Smallest time periods (day, week) allow for more variability in the data and hence provide more power to estimate the effects; however, they might not be capturing exactly the effects we are interested in. At short horizons, the estimate of β reflects how dwell time responds to transient fluctuations in water level — a short-term disruption to port operations rather than an adaptation to persistently different conditions. Climate change, by contrast, operates through a shift in the long-run average water level, to which ports can gradually adjust. Looking at changes in average water level over longer time periods (month, quarter) is conceptually closer to this counterfactual, as β then captures co-movement between dwell time and water level at a horizon where medium-run adjustments have had time to materialize — but the estimates might be less accurate due to less variability in the treatment.

Table 1: Effect of average water level on port average dwell time

	(1) t = day	(2) t = week	(3) t = month	(4) t = quarter
water level in port i	0.0217***	0.0348***	0.0813**	0.1153**
	(0.0033)	(0.0069)	(0.0317)	(0.0544)
# observations	1,994,540	520,533	146,081	53,183
# ports	1,679	1,679	1,679	1,679

Standard errors (clustered by port) in parentheses.
* $p < 0.10$, ** $p < 0.05$, *** $p < 0.01$

Results in Table 1 show a significant effect of water level on port dwell time, consistent with higher water levels disrupting port operations and delaying vessel processing. The point estimates increase with the length of the time period considered. A +1m increase in average water level over a quarter (equal to around 1.25 standard deviations) increases average dwell time over that quarter by approximately 12.2%.

Additional results Instead of accounting linearly for water level, I can consider discrete bins of water level, to capture potential non-linear effects. I consider either absolute bins thresholds, based on the distribution of water level over all ports (0.65m, 1.95m, 3.90m corresponding to percentiles 50, 90 and 99 of port daily observations over the 2015-2023 period), or relative bins thresholds based on port-specific distributions of water level over the period.[7] Results in Tables B.3 and B.4 show a consistent pattern: the effect of water level is mostly driven by extreme events, when water level is *very* high. The linear specification might then understate the effect of water level shocks, as it smooths the potential extreme events happening within a period. However, I keep the linear specification as the preferred one since it better represents the effect of climate change according to the IPCC, which predicts an increase in average sea level but does not include an increase in water level variability with high confidence in its scenarios (Pörtner et al., 2019). To the extent that rising average levels will nonetheless shift the distribution of water level rightward, pushing more observations into the extreme tail, the linear estimate is conservative: it captures the effect of a mean shift under the assumption that the shape of the distribution remains unchanged, and therefore likely understates the true long-run effect of climate change on port dwell time.

Izaguirre et al. (2021) show the effect of several dimensions of weather on port operations. As a robustness exercise, I look at the effect of wave height, wind speed, and total precipitation on port dwell time, in addition to water level, all computed from ERA-5 reanalysis data. To make the results comparable across measures, I standardize all variables so that coefficients describe the effect of a +1 standard deviation shock. Results in B.1 show that the effects of the different weather measures are statistically indistinguishable from one another, with water level carrying the largest point estimate, followed by wave height, wind speed, and precipitation. This consistency across weather dimensions supports the validity of the baseline specification. While the effects are broadly comparable across weather dimensions, wave height yields the most precisely estimated effect (p-value $< 1\%$), reflecting its higher within-port variability across periods. Since wave height is not projected to increase significantly with climate change, water level remains the policy-relevant variable of interest. However, the greater precision of wave height estimates makes it a useful instrument for isolating the mechanisms through which weather shocks affect port efficiency, which I exploit in additional specifications below.

Shipping data also allow measure port efficiency through the entering traffic (Brancaccio et al., 2024), measured as the number of entry port calls (weighted by the ships capacity). Section B.2 reports the effect of water level on port entering traffic across time horizons. At the daily level, higher water levels significantly reduce entering traffic, consistent with vessels delaying port entry during adverse conditions. The effect vanishes at intermediate horizons, suggesting that traffic

[7] This latter specification is not subject to the *binning bias* identified by Jones et al. (2026), since each port is only compared to its own range of weather shocks.

volumes recover quickly after short-run disruptions. The annual estimate is negative and large, consistent with a longer-run reallocation of traffic away from persistently high water level ports.

To decompose further the effect at the daily level, I consider in appendix B.4 an event-study setting. It shows that weather shocks (days with extremely high water level or waves) increase the port dwell time on the exact day they happen, but also during the days before and after. The entering traffic also declines in advance of the shock – however, as made clear by wave height shocks, there seems to be a slight catch-up in the days after the shock, with more entering traffic. This is consistent with the quick traffic volumes recover after short-run disruptions, observed above.

Appendix B.5 performs similar reduced-form exercises at the *ship* level, rather than aggregating by port. The results are consistent, worse weather in a port increasing the dwell time of all ships entering into this port. Specifications at the port level are preferred because they allow to observe two measures efficiency: (average) dwell ship time and port traffic. At the ship level, one might only look at dwell time and hence only observe the intensive margin of weather of port efficiency (how long ships spend in the port), not the extensive margin (whether ships actually go into the port).

In appendix B.6, I additionally show that weather *inside* a port might have an effect on ships behavior *outside* of ports: when a port is disrupted, ships might prefer to wait outside of the port (to avoid paying additional port fees). I indeed find that bad weather in origin or departure port increases the trip duration of ships. This suggests once again that the effects observed in the ports might be only a lower bound of the full effects, since they do not capture ships waiting outside of ports.

An important consideration is why weather conditions *in ports* warrant greater analytical emphasis than those encountered *at sea* during the transit between ports. While it is true that vessels typically spend a larger share of their voyage at sea – where they may be exposed to adverse phenomena such as storms, high waves, and strong winds – maritime navigation allows for considerable flexibility. In particular, vessels can adjust their course in response to meteorological forecasts, a practice commonly referred to as weather routing. In contrast, ports are geographically fixed and thus more vulnerable to local weather disruptions. In addition, the adverse effects of weather shocks in ports are amplified by infrastructure constraints leading to congestion, while the open sea is unconstrained by physical infrastructure. To empirically assess the differential importance of weather conditions in ports versus those along the maritime route, I conduct a comparative analysis of their effects on shipping duration in Appendix B.7. The results indicate that adverse weather in ports has a more pronounced effect on shipping times, as it influences both port dwell times and the duration of journeys between ports.

3.2.2 Adaptation mechanisms

The reduced-form evidence of direct weather effect on port efficiency exploits short-run weather shocks. However, in the long run, these short-run weather shocks might trigger some reactions in ports and in the shipping network. The following reduced-form exercises aim at shedding light on these potential adaptation mechanisms taking place in ports and in the shipping network.

Heterogeneity among ports To examine whether ports adapt to persistently higher water levels, I augment the baseline specification with an interaction between the period weather and the port's long-run average climate, measured following **?** as the period-average weather:

$$\ln(\text{time})_{it} = \alpha + \beta_1 \ \text{waterlevel}_{it} + \beta_2 \ \text{waterlevel}_{it} \times \text{climate}_i + \delta_i + \delta_t + \epsilon_{it} \tag{2}$$

In this specification, the coefficient β_1 captures the effect of a transient water level shock, while β_2 captures whether this effect is attenuated for ports that are systematically exposed to higher water levels on average over the period. Given the direct effect of water level on dwell time established above, I expect β_1 to be positive; if there is some adaptation of ports, then β_2 would be negative. Results in Table 2 confirm these intuitions: both β_1 and β_2 are significant at the day and week levels, and β_1 is positive while β_2 is negative. This indicates that ports facing higher long-run average water levels are less sensitive to a temporary water level increase. This cross-section heterogeneity is consistent with adaptation: ports operating in persistently harsher environments seem to develop practices or infrastructure that buffer the impact of short-run shocks. The magnitude is meaningful: the negative interaction partially but not fully offsets the direct effect, suggesting adaptation is present but incomplete.

Table 2: Effect of average water level on port average dwell time, with climate heterogeneity

	(1)	(2)
	t = day	t = week
water level in port i	0.0407***	0.0631***
	(0.0065)	(0.0124)
water level in port i × period-avg	-0.0082***	-0.0122***
	(0.0021)	(0.0035)
# observations	1,994,540	520,533
# ports	1,679	1,679

Standard errors (clustered by port) in parentheses

* $p < 0.10$, ** $p < 0.05$, *** $p < 0.01$

Traffic diversion within the network Goods traveling from origin port i to destination port j can take multiple routes through intermediate ports. When adverse weather raises the cost of

transiting certain ports, traffic may divert to alternative routes – particularly away from those intermediate ports most exposed to climate events. To test for this mechanism, I estimate the following specification:

$$\text{share traffic}_{r,ij,t} = \alpha + \beta \ \text{waterlevel int.ports}_{r,ij,t} + \delta_r + \delta_{ij} + \delta_t + \epsilon_{it} \tag{3}$$

for a route r connecting ports i to j in period t. The dependent variable, share traffic$_{r,ij,t}$, measures the share of traffic between i and j going through route r during period t (in percentage).[8] The key regressor, waterlevel int.ports$_{r,ij,t}$, is the average water level at the intermediate ports along route r between i and j (excluded) during period t. The specification includes route, origin-destination, and period fixed effects. The time periodt is defined at the month, quarter, or annual level.[9]

Table 3 presents the results, which reveal a pronounced traffic substitution effect. A one standard deviation increase in the annual average water level in intermediate ports of route r (0.7m) reduces r's share of traffic between i and j by 0 percentage points. The effect grows with the length of the time horizon t, consistent with an adaptation mechanism: as intermediate ports become costlier to transit due to elevated water levels, shippers gradually reroute cargo to avoid them. Appendix table B.9 confirms the robustness of these findings to additional controls and fixed effects.

Table 3: Effect of water level in intermediate ports on traffic share along a route

	(1)	(2)	(3)
	t = month	t = quarter	t = year
water level in intermediate ports	-1.4668***	-2.4366***	-13.0468***
	(0.1787)	(0.3537)	(2.8259)
# observations	1,847,662	793,361	152,423
# routes	234,290	157,669	51,362

Standard errors (clustered by route r) in parentheses

* $p < 0.10$, ** $p < 0.05$, *** $p < 0.01$

The empirical analysis establishes a direct effect of weather on port efficiency: higher water levels increase the time ships spend in port, thereby raising transportation costs. The IPCC Pörtner et al. (2019) projects substantial water level rise in the coming decades, with heterogeneous exposure across ports worldwide. Estimating the long-run effects of such a shift requires accounting for the adaptation mechanisms that will inevitably accompany it. The reduced-form evidence points to two such channels: ports themselves may adapt their operations, and shipping may reorganize, rerouting traffic away from ports most affected by high water levels. I now embed

[8] I consider all the routes connecting i to j in the shipping data with less than 5 intermediate ports.

[9] Since this mechanism is an adaptation to shocks affecting ports, I do not expect to see effects over short time periods.

these mechanisms in a structural model of trade with shipping to quantify the global welfare impact of a permanent increase in average water levels.

4 Economic Geography Model with Shipping

The reduced-form evidence shows that port efficiency is affected by weather shocks, and that these effects propagate through the shipping network. To understand better the spillovers mechanism and estimate the global effect of weather shocks, I use an economic geography model of trade with shipping. I rely on the workhorse model of Allen & Arkolakis (2022) (A&A henceforth), designed to study road or rail transportation between cities, and adapt it to an international trade and shipping setting. I present the model below, highlighting the differences from A&A. In the presentation of the model, I abstract from time subscripts t for clarity, but I consider that this static model can be repeated over time.

4.1 Model set up

Consider a finite number of countries $c \in \{1, ..., C\} \equiv \mathcal{C}$, inhabited by $\bar{L}$ individuals, and a finite number of ports $i \in \{1, ..., N\} \equiv \mathcal{N}$ $(N > C)$.[10] The ports are located in countries – countries can have between zero and several ports. The countries are populated by individuals (resp. firms), who can locate in different regions of the country; they are related to the closest port of their region from which they can import and consume (resp. produce and export) goods. Each port thus has a catchment area where are located individuals and firms related to this port. Let $\omega_{c,i}$ denote the share of individuals and firms of country c that belong to port i catchment area.

Ports $i \in \mathcal{N}$ are connected by a transportation (shipping) network, represented by two matrices:

- a $N \times N$ matrix of links prices $\mathbf{T} = [t_{kl} \geq 1]$, where t_{kl} is the ad valorem (iceberg) cost of moving directly from $k \in \mathcal{N}$ to $l \in \mathcal{N}$ along a link.
- a $N \times 1$ matrix of nodes prices $\mathbf{P} = [p_k \geq 1]$, where p_k is the ad valorem cost incurred from going through port $k \in \mathcal{N}$.

Goods move from an origin port i to a destination port j through a route r, defined as a sequence of links and intermediate nodes connecting i to j. A route of length K from i to j is a sequence of $K + 1$ locations and the links in between: $r \equiv \{r_0 = i, r_1, ..., r_K = j\}$. Since iceberg

[10] In the original A&A model, there is an isomorphism between regions c and transport nodes i are they consider cities. Here, I introduce the distinction between the two as I am considering trade between countries but transportation between ports.

costs are multiplicative, the total cost of route r is

$$p_i \times t_{i,k_1} \times p_{k_1} \times t_{k_1,k_2} \times ... \times t_{k_{K-1},j} \times p_j = \underbrace{\left(\prod_{l=0}^{K} p_{r_l}\right)}_{\text{cost of nodes}} \underbrace{\left(\prod_{l=1}^{K} t_{r_{l-1},r_l}\right)}_{\text{cost of links}} \tag{4}$$

There are multiple routes going from origin i to destination j: let $\mathcal{R}_{ij}$ denote their set.

Goods are traded across port catchment areas (also referred to as locations). In this international setting, labor is considered to be immobile between locations.[11] Each individual related to port catchment area $i \in \mathcal{N}$ supplies one unit of labor inelastically (labor being the only factor of production) for a wage w_i. Individuals also purchase quantities of a continuum of goods $\nu \in [0,1]$ with constant elasticity of substitution σ. Let Y^W denote the total income in the economy. In what follows, average per capita income is taken as the numeraire: $Y^W/\bar{L} = 1$.

Each location $i \in \mathcal{N}$ is endowed with a constant return to scale technology for producing and shipping each good $\nu \in [0,1]$ to each destination $j \in \mathcal{N}$ along each route $r \in \mathcal{R}_{ij}$. The technology is origin-destination-route specific, subject to idiosyncratic shocks $\epsilon_{ij,r}(\nu)$ – following Eaton & Kortum (2002), $\epsilon_{ij,r}(\nu)$ is independently and identically Fréchet-distributed across routes and goods, with a scale parameter $1/\bar{A}_i$ (capturing origin-specific efficiency) and a shape parameter θ (regulating the shock dispersion).

Under perfect competition, the price in destination j of a good sourced in origin i and shippped along route r is given by

$$p_{ij,r}(\nu) = w_i \frac{\left(\prod_{l=0}^{K} p_{r_l}\right)\left(\prod_{l=1}^{K} t_{r_{l-1},r_l}\right)}{\epsilon_{ij,r}(\nu)} \tag{5}$$

Individuals in location j purchase each good $\nu \in [0,1]$ from the cheapest source (i.e. origin-route).

4.2 Gravity and equilibrium

Following closely A&A, given the Fréchet distribution of origin-destination-route specific productivities, the probability that $j \in \mathcal{N}$ purchases good $\nu \in [0,1]$ from $i \in \mathcal{N}$ along route $r \in \mathcal{R}_{ij}$ can

[11] As opposed to A&A setting that considers cities within a country, where labor is perfectly mobile.

be written as:

$$\pi_{ij,r} = \frac{\left(w_i/\bar{A}_i\right)^{-\theta}\left(\prod_{l=0}^{K} p_{r_l}^{-\theta}\right)\left(\prod_{l=1}^{K} t_{r_{l-1},r_l}^{-\theta}\right)}{\sum_{k\in\mathcal{N}}\left(w_k/A_k\right)^{-\theta}\sum_{r'\in\mathcal{R}_{kj}}\left(\prod_{l=0}^{K} p_{r'_l}^{-\theta}\right)\left(\prod_{l=1}^{K} t_{r'_{l-1},r'_l}^{-\theta}\right)} \tag{6}$$

The total value of goods shipped from i to j, X_{ij} is obtained by summing across all routes r connecting i to j. As in Eaton & Kortum (2002), the probability of purchasing a good is equal to the expenditure share, yielding

$$X_{ij} = \sum_{r\in\mathcal{R}_{ij}} \pi_{ij,r} E_j = \frac{(w_i/\bar{A}_i)^{-\theta}\tau_{ij}^{-\theta}}{\sum_{k\in\mathcal{N}}(w_k/\bar{A}_k)^{-\theta}\tau_{kj}^{-\theta}} E_j \tag{7}$$

where τ_{ij} is the transportation cost from i to j – with an additional nodes cost term compared to A&A:

$$\tau_{ij} \equiv \left(\sum_{r\in\mathcal{R}_{ij}}\left(\prod_{l=0}^{K} p_{r_l}^{-\theta}\right)\left(\prod_{l=1}^{K} t_{r_{l-1},r_l}^{-\theta}\right)\right)^{-\frac{1}{\theta}} \tag{8}$$

Market clears at the equilibrium: total income Y_i in each location is equal to its total sales, and total expenditure E_i is each location is equal to its total purchases:

$$Y_i = \sum_{j=1}^{N} X_{ij}\ , \quad E_i = \sum_{j=1}^{N} X_{ji}, \tag{9}$$

Under these conditions, one can then retrieve the usual gravity equation:

$$X_{ij} = \tau_{ij}^{-\theta} \times \frac{Y_i}{\Pi_i^{-\theta}} \times \frac{E_j}{P_j^{-\theta}} \tag{10}$$

where Π_i and P_j are the market access terms (or multilateral resistance terms) as in Anderson & Van Wincoop (2003). Π_i is a producer price index capturing the (inverse) producer market access, while P_j is the consumer price index capturing the (inverse) consumer market access terms:

$$\Pi_i \equiv \left(\sum_j \tau_{ij}^{-\theta} E_j P_j^{\theta}\right)^{-\frac{1}{\theta}}, \quad P_j \equiv \left(\sum_i \tau_{ij}^{-\theta} Y_i \Pi_i^{\theta}\right)^{-\frac{1}{\theta}} \tag{11}$$

I introduce the same notations as A&A and define $y_i \equiv Y_i/Y^W$ and $l_i \equiv L_i/\bar{L}$ as the share of total income and total labor in location $i \in \mathcal{N}$, respectively. As opposed to A&A, labor is immobile: l_i is thus exogenously determined ($l_i = \bar{l}_i$) and there is no equalization of welfare across locations.

In this international trade setting, I assume that trade is imbalanced:[12] denoting D_i the deficit, $E_i = Y_i + D_i$ (with $\sum_i D_i = 0$). I further assume that the deficit is a share of local outcome, as in Costinot & Rodríguez-Clare (2014): $D_i = \kappa_i Y_i$. Hence

$$E_i = (1 + \kappa_i) Y_i \tag{12}$$

Combining these equations[13], I obtain the following equilibrium conditions:

$$\bar{A}_i^{-\theta} \bar{l}_i^{-\theta} y_i^{1+\theta} = \sum_j \tau_{ij}^{-\theta} (1 + \kappa_j) y_j P_j^{\theta} \tag{13}$$

$$P_i^{-\theta} = \sum_j \tau_{ji}^{-\theta} \bar{A}_j^{\theta} \bar{l}_j^{\theta} y_j^{-(\theta+1)} \tag{14}$$

Given $\{\bar{A}_i\}$, $\{\bar{l}_i\}$, $\{\tau_{ij}\}$, $\{\kappa_i\}$, 13 and 14 constitute a system of $2N$ equations can be solved to get equilibrium $\{y_i\}$ and $\{P_i\}$. However, similarly to A&A, I want to make the transportation costs endogenous, through traffic congestion on nodes and economies of scale on link, so that they also respond to the equilibrium distribution of y_i and P_i.

4.3 Endogenous transportation costs and weather

The first step is to write an analytical relationship between (i) transportation network characterized by links and nodes costs t_{ij} and p_i, and (ii) transportation costs τ_{ij}. I follow and adapt A&A procedure: starting from $\tau_{ij}^{-\theta} = \sum_{r \in \mathcal{R}_{ij}} \left(\prod_{l=0}^{K} p_{r_l}^{-\theta} \right) \left(\prod_{l=1}^{K} t_{r_{l-1}, r_l}^{-\theta} \cdot x_{r_{l-1}, r_l} \right)$ (equation 8) and enumerating all possible routes,[14] it comes that

$$\tau_{ij}^{-\theta} = \sum_{K=0}^{+\infty} (\mathbf{D}^K)_{ij} \; p_i^{-\theta}$$

where $\mathbf{D}$ is the $N \times N$ matrix of general term $d_{ij} \equiv t_{ij}^{-\theta} x_{ij} p_j^{-\theta}$, and $(\mathbf{D}^K)_{ij}$ is the term of the i-th and j-th column of matrix $\mathbf{D}$ to the power K. Provided that the spectral radius of $\mathbf{D}$ is less than one, the geometric sum can be expressed as:

$$\sum_{K=0}^{+\infty} \mathbf{D}^K = (\mathbf{I} - \mathbf{D})^{-1} \equiv \mathbf{C}^D$$

where $\mathbf{C}^D = \left[c_{ij}^D \right]$ is the Leontief inverse of the $\mathbf{D}$ matrix. As a result, the transportation cost from i to j can be written as a function of the transportation network:

[12] A&A consider balanced trade between cities; however in international trade data, expenditures are not equal to income, i.e. countries operate either in surplus or in deficit in a given year.

[13] See Appendix A.1 for detailed derivation of the equilibrium conditions.

[14] See Appendix A.2 for detailed derivation of the analytical relationship between τ_{ij}, t_{ij} and p_i.

$$\tau_{ij}^{-\theta} = c_{ij}^{D}\, p_i^{-\theta} \tag{15}$$

Once there is an analytical relationship between transportation network and transportation costs, the next step is to make the transportation network depend on traffic. Adapting A&A setting from *links* to *nodes*, I characterize the expected number of times in which a node k is used in trade between i and j, π_{ij}^{k}:

$$\pi_{ij}^{k} = \sum_{r \in \mathcal{R}_{ij}} \left(\frac{\pi_{ij,r}}{\sum_{r' \in \mathcal{R}_{ij}} \pi_{ij,r'}} \right) n_r^k \tag{16}$$

which can be rewritten as:[15]

$$\pi_{ij}^{k} = \frac{\tau_{ik}^{-\theta}\; p_k^{\theta}\; \tau_{kj}^{-\theta}}{\tau_{ij}^{\theta}} \tag{17}$$

This equation is close to Allen & Arkolakis (2022) as I can isolate a cost on the left of the node, the cost of the node, a cost on the right of the node. The third term of the equation might be confusing because of the positive exponent on p_k: this is because p_k already enters (negatively) in both τ_{ik} and τ_{kj}, so it is double counted.

Let Ξ_k be the node traffic in location k, i.e. the value of all goods going through node k (either because they have k as an origin or destination, or just because they transit through k as an intermediate node along their route):

$$\Xi_k = \sum_{i \in \mathcal{N}} \sum_{j \in \mathcal{N}} \pi_{ij}^{k} X_{ij} \tag{18}$$

This expression can be written as gravity equation for node traffic, with the same market access terms as a the gravity equation for trade flows 10:

$$\Xi_k = p_k^{\theta} \times P_k^{-\theta} \times \Pi_k^{-\theta} \tag{19}$$

A&A also show that similarly, link traffic Ξ_{kl} can be expressed with a gravity equation for link traffic:

$$\pi_{ij}^{kl} = \frac{\tau_{ik}^{-\theta}\; t_{kl}^{-\theta} x_{kl}\; \tau_{lj}^{-\theta}}{\tau_{ij}^{\theta}} \tag{20}$$

$$\Xi_{kl} = t_{kl}^{-\theta} x_{kl} \times P_k^{-\theta} \times \Pi_l^{-\theta} \tag{21}$$

With (i) the analytical relationship between transportation cost τ_{ij} and network costs t_{ij}, p_i given by 15, and (ii) expressions of traffic given by 19 and 21, I can now introduce congestion by

[15] See Appendix A.3 for detailed derivation of traffic expressions.

making the network costs t_{ij}, p_i depend on traffic – which will ultimately impact transportation cost τ_{ij}. Differently from A&A, to better represent shipping transportation (while they focus on railroads or highway transportation) I do not introduce traffic congestion on the *links* but rather on the *nodes* of the transportation network. Following insights from Ganapati et al. (2021), I also allow for economies of scales on the links.

I allow link costs t_{kl} to depend endogenously on traffic, motivated by well-documented economies of scale in maritime shipping. A first source of economies of scale is technological: larger vessels have substantially lower per-unit operating costs, as fuel, crew, and port time are spread over more containers. Crucially, larger and more cost-efficient vessels can only be deployed on routes with sufficient traffic to fill them. A second source is operational: running a shipping service on link kl requires committing a vessel to that route (paying for the crew, port fees at both ends, and the capital cost of the ship) regardless of how many containers fill it. These fixed costs must be recovered from the containers that use the link. When traffic is high, they are spread over many containers and the per-container contribution is negligible. When traffic is low, the few containers effectively bear the entire fixed cost of the voyage, making shipping prohibitively expensive. Together, these two forces imply that the per-unit cost of shipping a container on link kl is decreasing in the volume of traffic on that link, generating a self-reinforcing mechanism: the more traffic a link attracts, the cheaper it becomes to use, which in turn attracts more traffic. This naturally concentrates traffic on a small number of high-volume routes, rationalizing the sparse structure of the observed shipping network. Following the modeling philosophy of Arkolakis (2010), who rationalizes the extensive margin of firm exports through a smooth variable cost function rather than a discrete fixed cost of entry, I capture the reduced-form implication of these economies of scale directly through a per-unit iceberg cost that is decreasing in traffic, without modeling the shipping sector's optimization problem explicitly. Formally:

$$t_{kl} = \bar{t}_{kl} + \frac{1}{\alpha \Xi_{kl}} \tag{22}$$

where $\bar{t}_{kl}$ is the standard variable cost reflecting distance, fuel, and time at sea, and $\frac{1}{\alpha \Xi_{kl}}$ is the per-container incidence of fixed operating costs, decreasing in traffic Ξ_{kl}. The parameter $\alpha > 0$ governs the strength of economies of scale. When traffic Ξ_{kl} is large, the second term vanishes and the effective cost approaches the variable cost $\bar{t}_{kl}$, as in Allen & Arkolakis (2022). When traffic is small, the second term dominates and the link becomes effectively inactive, rationalizing the zeros observed in the data.

Quite the opposite, the cost of traveling through a node will depend negatively in this node's traffic because of congestion. More precisely, I follow Brancaccio et al. (2024) in assuming that

the cost of going through a port depends on the amount of time spent on this port:[16]

$$p_k = (\text{time}_k)^{\delta_0} \tag{23}$$

where time_k is the dwell time at port k and δ_0 is the time elasticity of the transportation cost. The time spent in a port depends in turn on the port's capacity and traffic:[17]

$$\text{time}_k = \omega_k \left(\frac{\Xi_k}{K_k} \right)^{\delta_1} \tag{24}$$

where ω_k is the productivity of port k (capturing for instance the labor force, productivity shocks...) and K_k the port capacity (number of ships that can be handled simultaneously, e.g. related to the number of berths). δ_1 is the congestion elasticity of time spent at port. Finally, the port capacity is affected by weather conditions – but the effect of weather on port capacity is heterogeneous:

$$K_k = \exp(\gamma_k \text{ weather}_k) \ \delta_k \tag{25}$$

where weather_k is a measure of weather at port k and δ_k captures other components of port capacity. γ_k captures the effect of weather on port k: this effect is port specific, as reduced-form evidence has shown that it can be heterogeneous. I follow Carleton et al. (2022) and assume that γ_k can depend on factors governing adaptation, in particular climate:

$$\gamma_k = \gamma^0 + \gamma^1 \text{ climate}_k \tag{26}$$

Combining equations 23, 24 and 25 yields

$$p_k = \omega_k^{\delta_0} \delta_k^{-\delta_0\delta_1} \exp(-\gamma_k \delta_0 \delta_1 \text{ weather}_k)(\Xi_k)^{\delta_0\delta_1} \quad \text{i.e.} \quad p_k = \bar{\Gamma}_k \exp(\mu_k \text{ weather}_k)(\Xi_k)^{\lambda} \tag{27}$$

Combining equation 27 with the gravity equation for node traffic 19 yields

$$p_k = \bar{\Gamma}_k^{\frac{1}{1-\lambda\theta}} \ e^{\frac{\mu_k}{1-\lambda\theta} \text{ weather}_k} \ P_k^{\frac{-\lambda\theta}{1-\lambda\theta}} \ \Pi_k^{\frac{-\lambda\theta}{1-\lambda\theta}} \tag{28}$$

Substituting equation 22 into the general term of the $\mathbf{D}$ matrix introduces an additive structure

[16] Brancaccio et al. (2024) show that the cost for a ship to stop in a port has a fixed amount (for port services) and an additional amount depending on the time spent in the port. Their descriptive statistics show that the time-depending part constitutes the majority of the total cost. They also notice that their estimate of time cost might be a lower bound as it only includes the cost of staying in the port, but not delays for the next transportation step nor the inventory costs that importers and exporters face. Relying on this, I neglect the fixed part of port cost to focus only on the time-depending part. Additionally, Brancaccio et al. (2024) show evidence of a convex relationship between time at port and traffic, which justifies the functional form in equation 23.

[17] This functional form is a simplification compared to Brancaccio et al. (2024) who assume that time $= T\left(1 + \mathbb{1}\{Q > K\}\frac{Q-K+1}{K}\right)$ where T the service time (depending on productivity of the port, labor, number of cranes...), Q the number of ships queuing, K the port capacity. In equation 24 I abstract from the distinction between the time ships spend queuing and being unloaded/reloaded.

in t_{kl} that is incompatible with the exact hat algebra approach: link costs no longer enter the $\mathbf{D}$ matrix multiplicatively, so the Leontief inverse trick of Allen & Arkolakis (2022) no longer applies analytically, and the equilibrium must be solved numerically in levels. Bringing this extension to the data further requires estimating the additional parameter α. For the remainder of the paper, I therefore abstract from economies of scale on links and set $t_{kl} = \bar{t}_{kl}$. Incorporating further the economies of scale on links and the resulting endogenous network structure into the quantification is work in progress.

$\bar{\boldsymbol{T}} = [\bar{t}_{kl}]$, $\boldsymbol{X} = [x_{kl}]$, and $\bar{\boldsymbol{\Gamma}} = \left[\bar{\Gamma}_k\right]$ describe the infrastructure network, exogenously given. $\lambda = \delta_0\delta_1 > 0$ is the congestion elasticity, $\mu_k = -\gamma_k\delta_0\delta_1 > 0$ is the weather elasticity. Equation 27 is similar to the endogenous link cost equation of A&A: the transportation cost endogenously depends on traffic – the key difference in my setting being that the congestion elasticity λ plays a role on the *nodes* cost (rather than the *links*). Fuchs & Wong (2024) also include node congestion in their model, in a similar fashion. The additional weather elasticity μ is a novelty compared to both Allen & Arkolakis (2022) and Fuchs & Wong (2024).

4.4 General equilibrium and exact hat algebra

Combining the equilibrium expressions 13 and 14 with equations 15, 21 and 28 allows to write the general equilibrium of the model with endogenous port costs.[18] Given a local geography $\{\bar{A}_i, \bar{l}_i\}_{i\in\mathcal{N}}$, an aggregate labor endowment $\bar{L}$, trade deficits $\{\kappa_i\}_{i\in\mathcal{N}}$, an infrastructure network $\bar{\boldsymbol{T}} = [\bar{t}_{kl}]$, $\boldsymbol{X} = [x_{kl}]$, and $\bar{\boldsymbol{\Gamma}} = \left[\bar{\Gamma}_k\right]$, a weather measure $\{\text{weather}_i\}_{i\in\mathcal{N}}$ and model parameters $\{\theta, \lambda, \mu_i\}_{i\in\mathcal{N}}$, the equilibrium is a distribution of economic activity $\{y_i, P_i\}_{i\in\mathcal{N}}$ satisfying:

$$\begin{aligned} y_i^{\theta+1+\frac{\lambda\theta(\theta+1)}{1-\lambda\theta}} P_i^{-\frac{\lambda\theta^2}{1-\lambda\theta}} =& \bar{L}^{-\frac{\lambda\theta}{1-\lambda\theta}} \bar{A}_i^{\frac{\lambda\theta^2}{1-\lambda\theta}+\theta} \bar{\Gamma}_i^{\frac{-\theta}{1-\lambda\theta}} e^{\frac{-\mu_i\theta}{1-\lambda\theta}\text{weather}_i} \bar{l}_i^{\frac{\lambda\theta^2}{1-\lambda\theta}+\theta} (1+\kappa_i) y_i P_i^{\theta} \\ &+ \bar{L}^{-\frac{\lambda\theta}{1-\lambda\theta}} \sum_{j=1}^{N} \bar{A}_i^{\frac{\lambda\theta^2}{1-\lambda\theta}+\theta} \bar{A}_j \bar{t}_{ij}^{-\theta} \bar{\Gamma}_i^{\frac{-\theta}{1-\lambda\theta}} e^{\frac{-\mu_i\theta}{1-\lambda\theta}\text{weather}_i} \bar{l}_i^{\frac{\lambda\theta^2}{1-\lambda\theta}+\theta} \bar{l}_j^{-\theta} y_j^{1+\theta} \end{aligned} \tag{29}$$

$$\begin{aligned} y_i^{\frac{\lambda\theta(\theta+1)}{1-\lambda\theta}} P_i^{-\theta-\frac{\lambda\theta^2}{1-\lambda\theta}} =& \bar{L}^{\frac{-\lambda\theta}{1-\lambda\theta}} \bar{A}_i^{\frac{\lambda\theta^2}{1-\lambda\theta}+\theta} \bar{\Gamma}_i^{\frac{-\theta}{1-\lambda\theta}} e^{\frac{-\mu_i\theta}{1-\lambda\theta}\text{weather}_i} \bar{l}_i^{\frac{\lambda\theta^2}{1-\lambda\theta}+\theta} y_i^{-\theta+1} \\ &+ \bar{L}^{-\frac{\lambda\theta}{1-\lambda\theta}} \sum_{j=1}^{N} \bar{A}_i^{\frac{\lambda\theta^2}{1-\lambda\theta}} \bar{t}_{ij}^{-\theta} \bar{\Gamma}_i^{\frac{-\theta}{1-\lambda\theta}} e^{\frac{-\mu_i\theta}{1-\lambda\theta}\text{weather}_i} \bar{l}_i^{\frac{\lambda\theta^2}{1-\lambda\theta}} P_j^{-\theta} \end{aligned} \tag{30}$$

To quantify the impact of a weather shock affecting ports infrastructure, I rely on the standard exact hat algebra approach and write the model in terms for changes from the equilibrium – using the notations $\hat{e}_i \equiv \frac{e_i'}{e_i}$ and $\Delta e_i \equiv e_i' - e_i$ for any variable e.

[18] See Appendix A.5 for detailed derivation of the equilibrium equations.

Consider a change in weather $\{\Delta\text{weather}_i\}_{i\in\mathcal{N}}$ and a change in trade deficits $\{\widehat{(1+\kappa_i)}\}_{i\in\mathcal{N}}$[19]. Given observed link traffic flows $\{\Xi_{ij}\}$, economic activity $\{Y_i, E_i\}$, and model parameters $\{\theta, \lambda, \mu_i\}$, the equilibrium change in economic outcomes $\{\hat{y}_i, \hat{P}_i\}$ is the solution of the following system of equations:[20]

$$\begin{aligned}\hat{y}_i^{\frac{1+\theta}{1-\lambda\theta}}\hat{P}_i^{\frac{-\theta}{1-\lambda\theta}+\theta} = &\left(\frac{E_i}{E_i+\sum_j \Xi_{ij}}\right) e^{\frac{-\mu_i\theta}{1-\lambda\theta}\Delta\text{weather}_i}\widehat{(1+\kappa_i)}\hat{y}_i\hat{P}_i^{\theta} \\ &+\sum_{j=1}^{N}\left(\frac{\Xi_{ij}}{E_i+\sum_j \Xi_{ij}}\right) e^{\frac{-\mu_i\theta}{1-\lambda\theta}\Delta\text{weather}_i}\hat{y}_j^{\theta+1}\end{aligned} \tag{31}$$

$$\begin{aligned}\hat{y}_i^{\frac{\theta+1}{1-\lambda\theta}-(\theta+1)}\hat{P}_i^{\frac{-\theta}{1-\lambda\theta}} = &\left(\frac{Y_i}{Y_i+\sum_j \Xi_{ji}}\right) e^{\frac{-\mu_i\theta}{1-\lambda\theta}\Delta\text{weather}_i}\hat{y}_i^{-\theta} \\ &+\sum_{j=1}^{N}\left(\frac{\Xi_{ji}}{Y_i+\sum_j \Xi_{ji}}\right) e^{\frac{-\mu_i\theta}{1-\lambda\theta}\Delta\text{weather}_i}\hat{P}_j^{-\theta}\end{aligned} \tag{32}$$

5 Estimation: Congestion and Weather Elasticities

There are two key elasticities to estimate to take to model to the data: the congestion elasticity and the weather elasticity. I can derive an estimation equation for them from the model micro-foundations and take it to the shipping and weather data described above. Combining equations 24 and 25 leads to

$$\text{time}_i = \Xi_i^{\delta_1} e^{-\delta_1\left(\gamma^0+\gamma^1\ \text{climate}_i\right)\ \text{weather}_i}\omega_i^{\delta_1}\delta_i \tag{33}$$

Building on Fuchs & Wong (2024), I consider the following estimation equation:

$$\begin{aligned}\ln(\text{time}_{sit}) = &-\delta_1\gamma^0\ \text{weather}_{i,[t-X;\,t]} - \delta_1\gamma^1\ \text{weather}_{i,[t-X;\,t]}\times\ \text{climate}_i \\ &+\delta_1\ln(\Xi_{i,[t-X;\,t]}) + \delta_s + \delta_i + \delta_t + \epsilon_{sit}\end{aligned} \tag{34}$$

where s denotes a ship, i a port, and t a day. time_{sit} is the dwell time experienced by ship s in port i on day t. $\Xi_{i,[t-X;\,t]}$ is a moving average of traffic at port i over the X days before t. I consider traffic over the past days to capture the potentially long-lasting effects of congestion – since it is increasing the dwell time, it might propagate to the next days. Similarly, $\text{weather}_{i,[t-X;\,t]}$ is a moving average of weather at port i over the X days before t. I also consider weather over the past days for several reasons: 1/ reduced-form evidence have shown that weather shocks can have effects lasting after the actual event (Appendix B.4); 2/ since weather also affects dwell time indirectly through traffic (that is endogenous and depends on port costs, hence on local weather)

[19] With a slight abuse of notation: $\widehat{(1+\kappa_i)} = \frac{1+\kappa_i'}{1+\kappa_i}$

[20] See Appendix A.6 for detailed derivation of the exact hat algebra equilibrium equations.

and that I consider traffic over the past days, I also need to control for weather over this period. I add ship, port and day fixed-effects. The standard errors are clustered at the ship level. I set X = 14 days, but I find similar results using a longer time period for the moving averages (especially setting X = 28 as Fuchs & Wong 2024 do).

Following insights from reduced-form exercises, I measure weather as water level and account for the possibility of adaptation of port efficiency to the long run change in weather. I rely on Carleton et al. (2022) and add an additional regressor by interacting short the run water level with a long-run climate variable, the sample-period average water level:

$$\text{weather}_{i,[t-X;\,t]} = \text{waterlevel}_{i,[t-X;\,t]} \quad \text{and} \quad \text{climate}_i = \overline{\text{waterlevel}}_i$$

I expect the coefficient of the weather level variable to be positive, as bad weather increases port dwell time, but the coefficient of the weather $\times$ climate variable to be negative if there is adaptation to bad weather.

The measure of port traffic Ξ_{it} is defined as the number of ships present at the port i during day t, weighted by the share of the day the ships spend at the port[21] and by the ships capacity (vessel dead-weight tonnage).

There is an endogeneity issue with port traffic $\Xi_{i,[t-X;\,t]}$. The main threat to identification comes from potential reverse causality if the traffic is influenced by the time spent in port – for instance, when the dwell time begins to increase, ships might start to avoid the port, reducing traffic. Additionally, the unobserved shocks in the error term might affect both traffic and dwell time (productivity shocks for instance). To instrument for port traffic, I suggest use lagged port traffic: I consider port traffic at the exact same date, but one year before.

$$\mathbf{Z}_{i,[t-X;\,t]} = \ln(\Xi_{i,[t-X-1y;\,t-1y]}) \tag{35}$$

To be valid, this instrument needs to be relevant and exogenous. Relevance (i.e. $\mathbf{Z}$ correlated with Ξ) comes from seasonality in port traffic. Exogeneity requires that $\mathbf{Z}$ is correlated with the dwell time solely through its correlation with congestion Ξ. There seems to be no channel through which previous year traffic could directly influence this year dwell time.

Results are reported in Table 4. I consider three specifications: including only weather and climate among the regressors (column 1), including also traffic but not instrumenting for it (column 2), finally implementing the IV strategy (column 3). As expected, a high water level

[21] e.g. if a ship arrives very late in the day, it will not contribute as much to traffic this as a ship arrived very early in the day

Table 4: Effect of moving-average traffic and water level on port dwell time, accounting for climate heterogeneity

	(1)	(2) OLS	(3) IV
water level (MA)	0.06866***	0.04633***	0.04264***
	(0.00803)	(0.00805)	(0.00807)
water level (MA) × period-avg	-0.01471***	-0.00851**	-0.00748**
	(0.00353)	(0.00358)	(0.00359)
log traffic (MA)		0.18724***	0.21812***
		(0.00280)	(0.01463)
date FE	✓	✓	✓
ship FE	✓	✓	✓
port FE	✓	✓	✓
# observations	6,302,310	6,302,310	6,302,310
# ships	11,531	11,531	11,531
First Stage KP-F			4937.8

Standard errors in parentheses
* $p < 0.10$, ** $p < 0.05$, *** $p < 0.01$

event is associated with an increase in port dwell time, but this effect is mitigated when ports are exposed to higher water level on average over the long run. The OLS estimator of traffic elasticity is in the same order of magnitude as the one of Fuchs & Wong (2024) (I find 0.19 while there OLS estimate is 0.10), although I also include weather, consider a shorter moving average window and a more exhaustive set of ports. The instrument used in the IV specification seems sufficiently strong, as indicated by the high heteroskedasticity-robust Kleibergen-Paap rk Wald F statistic (KP-F). The IV value of traffic elasticity is very close to the one found by Fuchs & Wong (2024) using a different instrument (0.22 vs 0.24). In appendix C, I show results adding more fixed effects to the specification (ship-port and port-year) and two-way clustering the standard errors at the ship and port levels, following Fuchs & Wong (2024). I find qualitatively similar results but with lower significancy.

6 Sea Level Rise Counterfactuals

I now turn to counterfactuals. I first explain how I take the model to the data, then present the counterfactual exercises and their result.

6.1 Taking the model to the data

Structural parameters The estimation presented below allows to recover values of δ_1 and γ_0, γ_1, related respectively to the congestion and weather elasticities. I turn to the literature to get values of other structural parameters. I rely on Allen & Arkolakis (2022) for the value of θ: I

take $\theta = 8$ from Donaldson & Hornbeck (2016). I follow the same approach as Fuchs & Wong (2024) to set a value for δ_0, relying on Hummels & Schaur (2013): from their level-log elasticity of trade costs to transportation time, I derive a log-log elasticity of 0.4. Table 5 summarizes the parameters values used to compute the counterfactuals.

Table 5: Structural parameters values used in the counterfactuals computation

parameter	value	source
θ	8	Donaldson & Hornbeck (2016)
δ_0	0.4	Fuchs & Wong (2024); Hummels & Schaur (2013)
δ_1	0.22	estimation
λ	0.1	$\delta_0\delta_1$
γ_0, γ_1	-0.18, 0.03	estimation
μ_0, μ_1	$0,016$, $-0,003$	$-\gamma_0\delta_0\delta_1$, $-\gamma_1\delta_0\delta_1$

Port catchment areas I consider the top 400 container ports[22] and define their respective catchment areas. To do so, I start with a $0.25° \times 0.25°$ grid (representing cells of up to 30 km $\times$ 30 km at the Equator) covering all countries, weighted by population (CIESIN, 2018). Each grid cell is then assigned to the most relevant port based on the following rules:

1. if the country has ports, the cell is allocated to the closest domestic port;
2. if the country is landlocked, the cell is allocated to the closest land-accessible foreign port.

These rules reflect a preference for domestic ports, even when a foreign port may be geographically closer. Distances are computed using the Open Route Service API (OpenRouteService, 2025), which accounts for actual road networks rather than straight-line ("as-the-crow-flies") distances. This adjustment is crucial, especially in developing countries where sparse or indirect road networks can significantly increase travel distances. Additionally, I incorporate port importance into the catchment area calculation. Larger and better-equipped ports may attract more exports and imports, even when farther away. To account for this, I use total entering port calls over the 2015–2023 period as a proxy for port importance and adjust distances accordingly. Specifically, I scale the road distance to each port by $1/\sqrt{\text{port importance}}$. This formulation implies that if two ports are at the same location but one is twice as large as the other, its catchment area will be twice as extensive.[23] With this procedure, I compute port catchment areas, i.e. shares of land related to each port, plotted in Figure 5. A port catchment area can cover only a part of a

[22] The raw AIS data contain many ports that are not adapted for containerships, or that are in fact technical stops for ships (for fuel, maintenance...) but not ports, etc. I use a cleaned version of the dataset to only look at point identified as container ports.

[23] For example, without adjusting for port importance, I find that only 1% of Chinese exports would go through Shanghai, despite it being the world's largest port, because it is located in a region with many other ports. Incorporating port importance corrects for this distortion.

country (e.g. French ports cover each one a share of French territory), a whole country or even several countries (e.g. the port of Calcutta catchment area covers part of India but also Nepal and Bhutan).

Figure 5: Port catchment areas worldwide

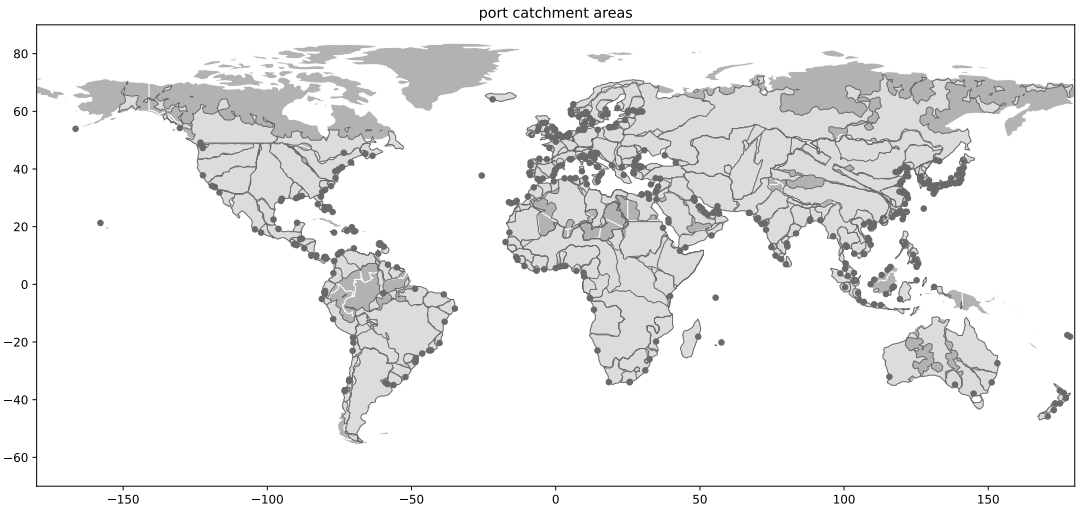

Note: Ports are plotted as dark dots, and port catchment areas are plotted as gray areas delimited by dark lines. The catchment area of a given port is the area in which this port is located. Parts of the world belong to no port catchment area because they have no road network to connect them to ports (e.g. the Amazon rainforest).

Outcome, expenditure, and traffic From the port catchment areas, I can compute the population-weighted shares of each country c related to each port i, $\omega_{c,i}$. I then rely on Penn World Tables to get country-level outcome Y_c and expenditure E_c for the year 2019. From these, I build port-level outcome $Y_i = \sum_c \omega_{c,i} Y_c$, representing the amount of goods produced by firms that export through port i (that can come from different countries); and port-level expenditure $E_i = \sum_c \omega_{c,i} E_c$, representing the amount of goods consumed by agents that import through port i (coming from potentially different countries as well).

To solve the exact hat algebra system of equations 31 and 31, I additionally require to observe traffic flows Ξ_{ij}. I take them from AIS shipping data, considering the shipping links that have more than 50 calls over the year 2019, between the 400 ports I take into account. For these links, I measure traffic Ξ_{ij} as the number of ships (weighted by their capacity) traveling on the link during the year 2019.

Outcome effects With these data and structural parameters values, I can compute the effects on endogenous variables of a given weather shock $\{\Delta\text{weather}_i\}_{i\in\mathcal{N}}$ following the exact hat algebra system of equations 31 and 32. I take trade deficits into account using a two-step procedure

(Ossa, 2016). I first compute counterfactual outcomes assuming no weather shock but taking the trade deficits to zero; then I compute counterfactuals with a weather change assuming the trade deficits stay to zero. The effect of the change in weather is computed as the difference between equilibrium levels in the two counterfactuals. This procedure is detailed in Appendix D. To solve the system of equations, I use a fixed point algorithm (adapted from the one of Allen & Arkolakis 2022, see Appendix E).

I retrieve the equilibrium changes in nominal economic outcome $\{\hat{y}_i\}_{i\in\mathcal{N}}$ and price index $\{\hat{P}_i\}_{i\in\mathcal{N}}$ at the port catchment area level, from which I can derive changes in real outcome $\{\hat{y}_i/\hat{P}_i\}_{i\in\mathcal{N}}$ – the reference welfare metric used by Arkolakis et al. (2012). To better understand the mechanisms leading to these welfare effects, I also look at the changes in port traffic $\{\hat{\Xi}_i\}_{i\in\mathcal{N}}$ and route traffic $\{\hat{\Xi}_{ij}\}_{i,j\in\mathcal{N}}$.

6.2 Predicted vs observed trade flows

As in Allen & Arkolakis (2022), there is a close link in the model between the gravity equation for trade flows (equation 10) and the gravity equation of traffic on links (equation 21). Combining these equations allows to write an expression of equilibrium trade flows as:[24]

$$X_{ij} = Y_i \times c_{ij}^X \times E_j \tag{36}$$

where c_{ij}^X is the (i,j)-th element of the matrix $\mathbf{C^X} \equiv \left(\mathbf{D^X} - [\Xi_{ij}]\right)^{-1}$, where $\mathbf{D^X}$ is a diagonal matrix with i-th element equal to $d_i^X \equiv \frac{1}{2}\left(Y_i + E_i\right) + \frac{1}{2}\left(\sum_j \Xi_{ij} + \Xi_{ji}\right)$.

Following Allen & Arkolakis (2022), this expression for traffic flows between locations i and j depends only on available data. It allows to build a *prediction* of trade flows based on the model, that we can then compare with *observed* trade flows from data, to check the validity of the model.

I rely on traffic flows between ports which catchment area does not cover several countries. From the traffic flows Ξ_{ij}, the outcome Y_i and expenditure E_i of those ports, I can predict trade flows at the *port level* X_{ij} using equation 36. I then aggregate ports to the country they belong to, to get predicted trade flows of the *country level* $X_{c,c'}$. I compare these model-precicted trade flows with bilateral trade flows data at the country level from Mayer et al. (2023) and Fontagné et al. (2023) in 2019 (aggregating all manufacturing and agriculture sectors together).[25]

[24] See Appendix A.4 for detailed derivation of the relationship between trade flows and traffic flows.

[25] Mayer et al. (2023) and Fontagné et al. (2023) combine data on annual cross-border international bilateral flows (UN Commodity Trade Statistics Database (COMTRADE) for manufacturing and Food and Agriculture Organization of the United Nations Statistics Division (FAOSTAT) for agriculture) with production data (the UNIDO Industrial Statistics database (INDSTAT) for manufacturing and again FAOSTAT for agriculture) to compile a square matrix of bilateral trade flows for each sector, including self-trade.

Figure 6: Predicted trade flows using traffic compared to observed trade flows

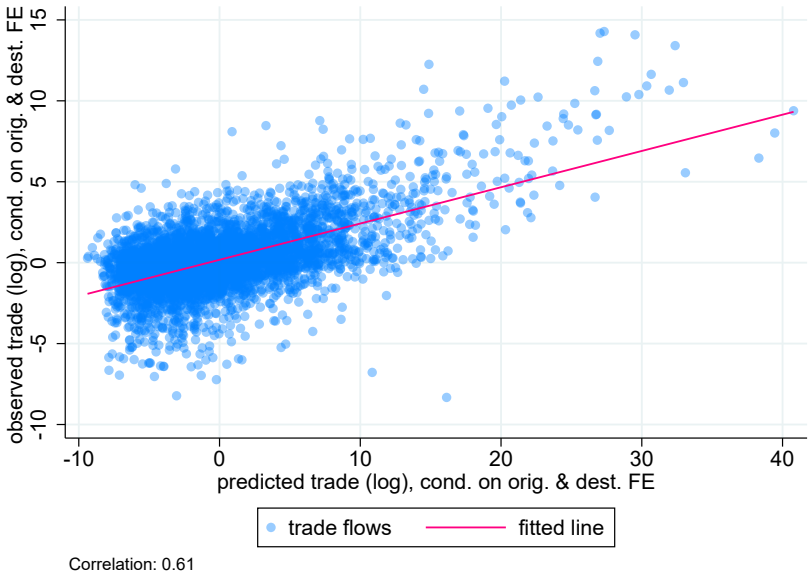

Figure 6 shows the scatter plot between observed and predicted log trade flows, conditional on origin and destination fixed effects.[26] The strong positive correlation (0.61) indicates that the traffic matrix is efficient in predicting the trade flows. This suggests the model is performing well to describe international trade flows with a shipping network, extending the result of Allen & Arkolakis (2022) showing that their original model performs well to describe trade between cities in US with a road network.

6.3 Counterfactuals: Sea Level Rise

I look at the effect of a global climate shock: sea level rise. In the coming years, all ports will experience a change in their water level; however, these changes will be heterogeneous, some ports will experience a much more important rise in water level than others (Pörtner et al., 2019). I compute the future water level at each port location using IPCC sea level projections (Garner et al., 2022) under the SSP5-8.5 scenario (very high GHG emissions). The counterfactual exercise computes the effects of the change in water level between 2019 and 2100 under this scenario.

$$\Delta \text{weather}_i = \text{water level}_{i,2019} - \text{water level}_{i,2100} \tag{37}$$

Figure 7 illustrates the changes in water level compared to 2019 at the different port locations.

[26] As Allen & Arkolakis (2022) notice, controlling for origin country and destination fixed effects allows that the variation arises only from the bilateral flows and not from characteristics of origin or destination countries such as income.

There is significant heterogeneity across ports: while some ports are expected to experience virtually no change in water level, most of the ports will experience sea level rise, up to +1.3m in 2100. Comparing these projections of future sea level rise after 2019 to realized sea level rise before 2019 from historical data, one can notice the acceleration in rising water level.

Figure 7: Evolution of water level in ports compared, using historical and projection data

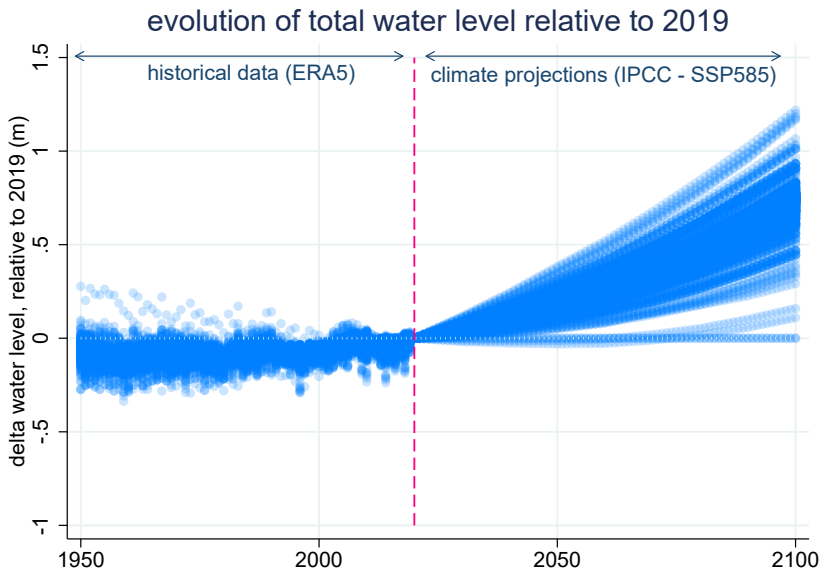

Note: each dot represents the change in total water level in one port, compared to 2019. Before 2019, the values are observed in ERA5 data. After 2019, the values are predicted by IPCC following the SSP5-8.5 scenario.

Figure 8 shows the spatial distribution of the changes in water level between 2019 and 2100. Some of the less affected ports locate in Northern Europe (Sweden, Norway, Finland) while the most affected ports are in the the Philippines and East Coast of the USA. The map also shows the significant spatial correlation of the sea level rise: ports in the same area are facing similar levels of water level increase.

The changes in local real outcome $\hat{y}_i/\hat{P}_i$ (i.e. welfare changes, Arkolakis et al. 2012) predicted by the model are presented in Figure 9. Ports loose up to 1.1% of real outcome, in Freeport (USA), New Orleans (USA), Subic Bay (Philippines), Manila (Philippines). The lowest impact is at -0.2% real outcome (Gavle, Sweden; Rauma, Finland).

Comparing maps 8 and 9, we see a correlation between the levels of water level increase and real outcome decrease: for instance, Northern Europe ports are among the less subject to sea level rise, and also suffer less welfare loss; quite the opposite, the Gulf of Mexico will experience both heavy sea level rise and welfare loss.

Figure 8: Changes in port water level between 2019 and 2100 under scenario SSP5-8.5

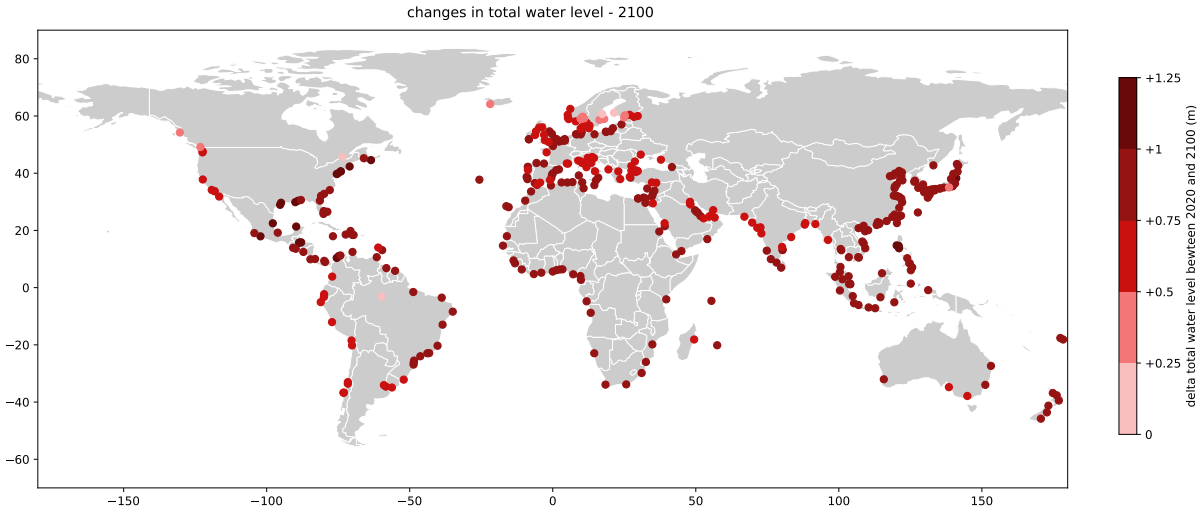

Figure 9: Changes in port real outcome between 2019 and 2100 under scenario SSP5-8.5

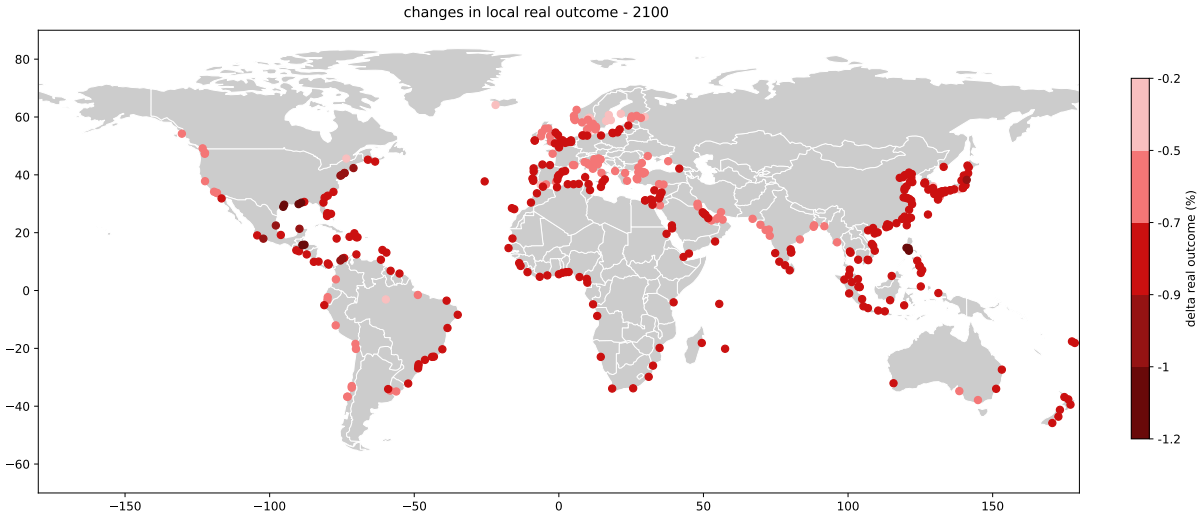

However, the mapping between local weather change and local welfare loss is not perfect. Looking closer at Europe (Figure 10), one can see ports with similar changes in water level (left panel) experiencing different changes in real outcome (right panel). For instance in Spain, the ports of Cadix and Barcelona experience very similar change in water level (resp. +0.80m and +0.81m) but quite different changes in real outcome (resp. -0.44% and -0.74%). This suggests that the impact of climate change on a given port cannot be determined by its own water level rise only (*direct* effect), spillovers from other ports (*indirect* effect) play a significant role.

Figure 11 displays the distribution of local water level changes and real outcome changes

Figure 10: Changes in water level and real outcome in 2100 – zoom on Europe

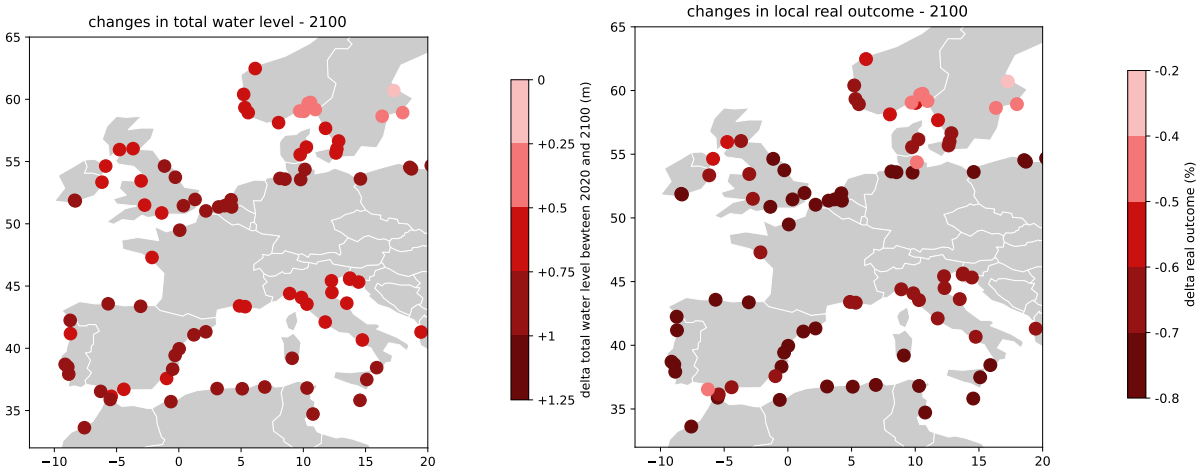

(a) change in water level (b) change in real outcome

Figure 11: Changes in local water level and real outcome at the port level under scenario SSP5-8.5

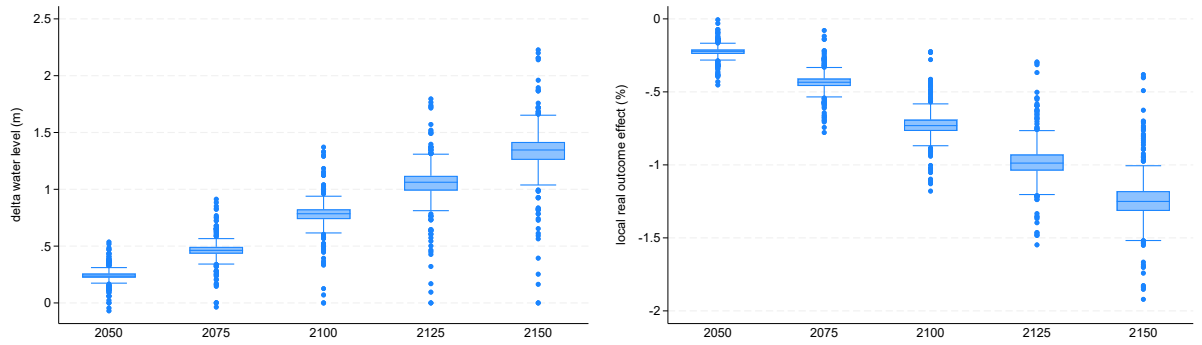

(a) water level (b) real outcome

across ports for different years under scenario SSP5-8.5. Two patterns stand out. First, the distribution of welfare losses widens over time, reflecting the compounding nature of climate impacts. Second, the figure illustrates the spillover mechanism: while some ports face no direct increase in water levels (left panel), all ports experience welfare losses (right panel). There is no port at zero in the welfare effects distribution: even ports that are entirely unaffected by local sea level rise suffer losses due to the indirect effects propagating through the shipping network from other ports.

7 Conclusion

I examine the economic impact of weather shocks affecting port infrastructures in the shipping network. I focus on the port congestion created by adverse weather conditions, that increases the cost of port services for ships. The framework provided allows to understand the spillovers mechanisms created by the network structure of shipping: the port inter-linkages spread the effect of local weather shocks, generating potential ripple effects – but also substitution mechanisms. I further show that the sparse structure of the shipping network can be rationalized through economies of scale on link costs, whereby links with insufficient traffic become prohibitively expensive and effectively inactive in equilibrium. Incorporating this mechanism into the quantification is work in progress; it will allow the network topology itself to respond endogenously to climate shocks, further amplifying the reallocation effects identified in the counterfactual exercises. A policy implication of this work is about infrastructure decisions to protect ports against sea level rise (Christodoulou et al., 2019): some ports are particularly critical for global welfare, and several countries would benefit from their protection.

References

Allen, T. & Arkolakis, C. (2014). Trade and the topography of the spatial economy. *The Quarterly Journal of Economics*, 129(3), 1085–1140.

Allen, T. & Arkolakis, C. (2022). The welfare effects of transportation infrastructure improvements. *The Review of Economic Studies*, 89(6), 2911–2957.

Anderson, J. E. & Van Wincoop, E. (2003). Gravity with gravitas: A solution to the border puzzle. *American economic review*, 93(1), 170–192.

Arkolakis, C. (2010). Market penetration costs and the new consumers margin in international trade. *Journal of political economy*, 118(6), 1151–1199.

Arkolakis, C., Costinot, A., & Rodríguez-Clare, A. (2012). New trade models, same old gains? *American Economic Review*, 102(1), 94–130.

Balboni, C., Boehm, J., & Waseem, M. (2023). Firm adaptation and production networks: Structural evidence from extreme weather events in pakistan.

Becker, A., Ng, A. K., McEvoy, D., & Mullett, J. (2018). Implications of climate change for shipping: Ports and supply chains. *Wiley Interdisciplinary Reviews: Climate Change*, 9(2), e508.

Brancaccio, G., Kalouptsidi, M., & Papageorgiou, T. (2020). Geography, transportation, and endogenous trade costs. *Econometrica*, 88(2), 657–691.

Brancaccio, G., Kalouptsidi, M., & Papageorgiou, T. (2024). Investment in infrastructure and trade: The case of ports. *National Bureau of Economic Research Working Paper*.

Carleton, T., Crews, L., & Nath, I. (2023). *Agriculture, trade, and the spatial efficiency of global water use*. Technical report, Working paper.

Carleton, T., Jina, A., Delgado, M., Greenstone, M., Houser, T., Hsiang, S., Hultgren, A., Kopp, R. E., McCusker, K. E., Nath, I., et al. (2022). Valuing the global mortality consequences of climate change accounting for adaptation costs and benefits. *The Quarterly Journal of Economics*, 137(4), 2037–2105.

Christodoulou, A., Christidis, P., & Demirel, H. (2019). Sea-level rise in ports: a wider focus on impacts. *Maritime Economics & Logistics*, 21, 482–496.

CIESIN (2018). Gridded population of the world, version 4.11 (gpwv4): Population count. Revision 11. Palisades, NY: NASA Socioeconomic Data and Applications Center (SEDAC).

Costinot, A., Donaldson, D., & Smith, C. (2016). Evolving comparative advantage and the impact of climate change in agricultural markets: Evidence from 1.7 million fields around the world. *Journal of Political Economy*, 124(1), 205–248.

Costinot, A. & Rodríguez-Clare, A. (2014). Trade theory with numbers: Quantifying the consequences of globalization. In *Handbook of international economics*, volume 4 (pp. 197–261). Elsevier.

Dell, M., Jones, B. F., & Olken, B. A. (2012). Temperature shocks and economic growth: Evidence from the last half century. *American Economic Journal: Macroeconomics*, 4(3), 66–95.

Deryugina, T., Kawano, L., & Levitt, S. (2018). The economic impact of hurricane katrina on its victims: Evidence from individual tax returns. *American Economic Journal: Applied Economics*, 10(2), 202–233.

Donaldson, D. & Hornbeck, R. (2016). Railroads and american economic growth: A "market access" approach. *The Quarterly Journal of Economics*, 131(2), 799–858.

Dube, A., Girardi, D., Jorda, O., & Taylor, A. M. (2023). *A local projections approach to difference-in-differences event studies*. Technical report, National Bureau of Economic Research.

Eaton, J. & Kortum, S. (2002). Technology, geography, and trade. *Econometrica*, 70(5), 1741–1779.

Fajgelbaum, P. D. & Schaal, E. (2020). Optimal transport networks in spatial equilibrium. *Econometrica*, 88(4), 1411–1452.

Fontagné, L., Lebrand, M. S. M., Murray, S., Santoni, G., & Ruta, M. (2023). Trade and infrastructure integration in africa. *Available at SSRN 4672520*.

Fuchs, S. & Wong, W. F. (2024). Multimodal transport networks. *Mimeo*.

Ganapati, S., Wong, W. F., & Ziv, O. (2021). Entrepot: Hubs, scale, and trade costs. *National Bureau of Economic Research Working Paper*.

Garner, G., Hermans, T. H., Kopp, R., Slangen, A., Edwards, T., Levermann, A., Nowicki, S., Palmer, M. D., Smith, C., Fox-Kemper, B., et al. (2022). Ipcc ar6 wgi sea level projections.

Gouel, C. & Laborde, D. (2021). The crucial role of domestic and international market-mediated adaptation to climate change. *Journal of Environmental Economics and Management*, 106, 102408.

Heiland, I., Moxnes, A., Ulltveit-Moe, K. H., & Zi, Y. (2019). Trade from space: Shipping networks and the global implications of local shocks. *CEPR Discussion Paper No. DP14193*.

Hersbach, H., Bell, B., Berrisford, P., Biavati, G., Horányi, A., Sabater, J. M., Nicolas, J., Peubey, C., Radu, R., Rozum, I., et al. (2023). Era5 hourly data on pressure levels from 1940 to present: Tech. rep.

Hummels, D. L. & Schaur, G. (2013). Time as a trade barrier. *American Economic Review*, 103(7), 2935–2959.

Izaguirre, C., Losada, I. J., Camus, P., Vigh, J. L., & Stenek, V. (2021). Climate change risk to global port operations. *Nature Climate Change*, 11(1), 14–20.

Jones, B., Moscona, J., Olken, B. A., & von Dessauer, C. (2026). *With or Without U? Binning Bias and the Causal Effects of Temperature Extremes*. Technical report, National Bureau of Economic Research.

Ludwig, P. (2024). Can unilateral policy decarbonize maritime trade?

Mayer, T., Santoni, G., & Vicard, V. (2023). *The CEPII trade and production database*. CEPII.

OpenRouteService (2025). Openrouteservice api documentation. https://openrouteservice.org. Heidelberg Institute for Geoinformation Technology. Accessed: 2025-02-26.

Ossa, R. (2016). Quantitative models of commercial policy. In *Handbook of commercial policy*, volume 1 (pp. 207–259). Elsevier.

Pörtner, H.-O., Roberts, D. C., Masson-Delmotte, V., Zhai, P., Tignor, M., Poloczanska, E., Weyer, N., et al. (2019). The ocean and cryosphere in a changing climate. *IPCC special report on the ocean and cryosphere in a changing climate*, 1155, 10–1017.

UNCTAD (2023). *Review of Maritime Transport*. Technical report.

Wang, D., Guan, D., Zhu, S., Kinnon, M. M., Geng, G., Zhang, Q., Zheng, H., Lei, T., Shao, S., Gong, P., et al. (2021). Economic footprint of california wildfires in 2018. *Nature Sustainability*, 4(3), 252–260.

Appendix

A Model derivations

A.1 Equilibrium equations

Combining equations 7 and 10 yields (using additionally that $Y_i = w_i L_i$):

$$\Pi_i = \bar{A}_i l_i y_i^{-\frac{\theta+1}{\theta}} \bar{L}^{1-\frac{\theta+1}{\theta}} \tag{A.1}$$

The market clearing condition $Y_i = \sum_j X_{ij}$ from 9 can be rewritten using 10 as

$$\Pi_i^{-\theta} = \sum_j \tau_{ij}^{-\theta} E_j P_j^{\theta} \tag{A.2}$$

With the unbalanced trade assumption 12, I can write the first equilibrium equation:

$$\bar{A}_i^{-\theta} \bar{l}_i^{-\theta} y_i^{1+\theta} = \sum_j \tau_{ij}^{-\theta} (1+\kappa_j) y_j P_j^{\theta} \tag{A.3}$$

Similarly, combining the market clearing condition $E_i = \sum_j X_{ji}$ from 9 with 10 yields

$$P_i^{-\theta} = \sum_j \tau_{ji}^{-\theta} Y_j \Pi_j^{\theta} \tag{A.4}$$

Here no need to account for deficit, it directly leads to the second equilibrium equation:

$$P_i^{-\theta} = \sum_j \tau_{ji}^{-\theta} \bar{A}_j^{\theta} \bar{l}_j^{\theta} y_j^{-(\theta+1)} \tag{A.5}$$

A.2 Transportation costs

Starting from $\tau_{ij}^{-\theta} = \sum_{r \in \mathcal{R}_{ij}} \left(\prod_{l=0}^{K} p_{r_l}^{-\theta} \right) \left(\prod_{l=1}^{K} t_{r_{l-1},r_l}^{-\theta} \right)$ (coming from equation 8), I follow A&A into enumerating all the possible routes going from i to j of length K :

$$\tau_{ij}^{-\theta} = \sum_{K=0}^{+\infty} \left(\sum_{k_1=1}^{N} \sum_{k_2=1}^{N} ... \sum_{k_{K-1}=1}^{N} p_i^{-\theta} t_{i,k_1}^{-\theta} p_{k_1}^{-\theta} t_{k_1,k_2}^{-\theta} ... p_{k_{K-1}}^{-\theta} t_{k_{K-1},j}^{-\theta} p_j^{-\theta} \right) \tag{A.6}$$

I then adapt the matrix algebra of A&A to simplify this expression. In equation A.6, one can group an origin port with the link after, i.e. consider $g_{ij} \equiv p_i^{-\theta} t_{ij}^{-\theta}$. In which case,

$$\tau_{ij}^{-\theta} = \sum_{K=0}^{+\infty} (\mathbf{G}^K)_{ij} \, p_j^{-\theta} \quad \text{then} \quad \sum_{K=0}^{+\infty} \mathbf{G}^K = (\mathbf{I} - \mathbf{G})^{-1} \equiv \mathbf{C}^G \quad \Rightarrow \quad \tau_{ij}^{-\theta} = c_{ij}^G \, p_j^{-\theta} \tag{A.7}$$

Another alternative to simplify equation A.6 is to group an origin port with the link before, i.e. consider $d_{ij} \equiv t_{ij}^{-\theta} p_j^{-\theta}$. Then,

$$\tau_{ij}^{-\theta} = \sum_{K=0}^{+\infty} (\mathbf{D}^K)_{ij}\, p_i^{-\theta} \quad \text{then} \quad \sum_{K=0}^{+\infty} \mathbf{D}^K = (\mathbf{I} - \mathbf{D})^{-1} \equiv \mathbf{C}^D \quad \Rightarrow \quad \tau_{ij}^{-\theta} = c_{ij}^D\, p_i^{-\theta} \tag{A.8}$$

Equations A.7 and A.8 provide two alternative analytical relationships between transportation network and transportation costs.

A.3 Traffic Gravity equations

Let π_{ij}^k denote the expected number of times in which a node k is used in trade between i and j, π_{ij}^k:

$$\pi_{ij}^k = \sum_{r \in \mathcal{R}_{ij}} \left(\frac{\pi_{ij,r}}{\sum_{r' \in \mathcal{R}_{ij}} \pi_{ij,r'}} \right) n_r^k \tag{A.9}$$

where n_r^k is the number of times the route r passes through node k. Combining with equation 6 yields:

$$\pi_{ij}^k = \tau_{ij}^{\theta} \left(\sum_{r \in \mathcal{R}_{ij}} \left(\prod_{l=0}^{K} p_{r_l}^{-\theta} \right) \left(\prod_{l=1}^{K} t_{r_{l-1},r_l}^{-\theta} \right) \right) n_r^k$$

I then enumerating explicitly all possible routes going from i to j through k. Routes can have different lengths K (equal to the number of links, or the number of ports -1). A route of length K can go through node k at position $B \in \{0, 1, ..., K\}$. Isolating the cost on the left of k and the cost on the right of k leads to:

$$\pi_{ij}^k = \tau_{ij}^{\theta} \sum_{K=0}^{\infty} \sum_{B=0}^{K-1} \left(\sum_{r \in \mathcal{R}_{ik,B}} \prod_{n=1}^{B} g_{r_{n-1},r_n} \right) p_k^{-\theta} \left(\sum_{r \in \mathcal{R}_{kj,K-B}} \prod_{n=1}^{K-B} d_{r_{n-1},r_n} \right)$$

Using the same computation tricks as above:

$$\pi_{ij}^k = \tau_{ij}^{\theta} \sum_{K=0}^{\infty} \sum_{B=0}^{K-1} (\mathbf{G}^B)_{ij}\, p_k^{-\theta}\, (\mathbf{D}^{K-B})_{ij} \tag{A.10}$$

With some matrix algebra, one can show that

$$\sum_{K=0}^{+\infty} \sum_{B=0}^{K-1} \mathbf{G}^B\, \mathbf{P}\, \mathbf{D}^{K-B} = (\mathbf{I} - \mathbf{G})^{-1}\, \mathbf{P}\, (\mathbf{I} - \mathbf{D})^{-1}$$

Using the notations from the equations A.7 and A.8:

$$\pi_{ij}^{k} = \frac{c_{ik}^{G}\, p_{k}^{-\theta}\, c_{kj}^{D}}{\tau_{ij}^{\theta}} = \frac{\tau_{ik}^{-\theta}\, p_{k}^{\theta}\, \tau_{kj}^{-\theta}}{\tau_{ij}^{\theta}} \tag{A.11}$$

Let Ξ_k be the node traffic in location k, i.e. the value of all goods going through node k (either because they have k as an origin or destination, or just because they transit through k as an intermediate node along their route):

$$\Xi_k = \sum_{i \in \mathcal{N}} \sum_{j \in \mathcal{N}} \pi_{ij}^{k} X_{ij} \tag{A.12}$$

Substituting for X_{ij} with equation 10, I find that equation A.12 can be written as gravity equation for node traffic, with the same market access terms as a the gravity equation for trade flows 10:

$$\Xi_k = p_k^{\theta} \times P_k^{-\theta} \times \Pi_k^{-\theta} \tag{A.13}$$

A&A also show that similarly, link traffic Ξ_{kl} can be expressed with a gravity equation for link traffic:

$$\pi_{ij}^{kl} = \frac{\tau_{ik}^{-\theta}\, t_{kl}^{-\theta}\, \tau_{lj}^{-\theta}}{\tau_{ij}^{\theta}} \tag{A.14}$$

$$\Xi_{kl} = t_{lk}^{-\theta} \times P_k^{-\theta} \times \Pi_l^{-\theta} \tag{A.15}$$

A.4 Traffic and trade

Writing equation 10 in matrix notations – where $[x_{ij}]$ denotes a $N \times N$ matrix of general term x_{ij}, and $\text{diag}\,(x_i)$ a $N \times N$ diagonal matrix where the diagonal term of the i-th row is equal to x_i:

$$[X_{ij}] = \text{diag}\left(\frac{Y_i}{\Pi_i^{-\theta}}\right) \left[\tau_{ij}^{-\theta}\right] \text{diag}\left(\frac{E_i}{P_i^{-\theta}}\right) \tag{A.16}$$

Combining with equation A.8, it yields

$$[X_{ij}] = \text{diag}\left(\frac{Y_i}{\Pi_i^{-\theta} p_i^{-\theta}}\right) (\mathbf{I} - \mathbf{D})^{-1} \text{diag}\left(\frac{E_i}{P_i^{-\theta}}\right) \tag{A.17}$$

with

$$\mathbf{D} = [d_{ij}] = \left[\tau_{ij}^{-\theta}\right] \text{diag}\left(p_i^{-\theta}\right)$$

It comes

$$[X_{ij}] = \text{diag}\left(\frac{Y_i}{\Pi_i^{-\theta} p_i^{-\theta}}\right) \left(\mathbf{I} - \left[\tau_{ij}^{-\theta}\right] \text{diag}\left(p_i^{-\theta}\right)\right)^{-1} \text{diag}\left(\frac{E_i}{P_i^{-\theta}}\right) \tag{A.18}$$

Similarly, writing equation 21 in matrix notations:

$$[\Xi_{ij}] = \text{diag}\left(P_i^{-\theta}\right)\left[t_{ij}^{-\theta}\right]\text{diag}\left(\Pi_i^{-\theta}\right) \tag{A.19}$$

Inverting, it comes:

$$\left[t_{ij}^{-\theta}\right] = \text{diag}\left(P_i^{\theta}\right)[\Xi_{ij}]\,\text{diag}\left(\Pi_i^{\theta}\right) \tag{A.20}$$

Combining equations A.18 and A.20:

$$[X_{ij}] = \text{diag}\left(\frac{Y_i}{\Pi_i^{-\theta}}p_i^{-\theta}\right)\left(\mathbf{I} - \text{diag}\left(P_i^{\theta}\right)[\Xi_{ij}]\,\text{diag}\left(\Pi_i^{\theta}\right)\text{diag}\left(p_i^{-\theta}\right)\right)^{-1}\text{diag}\left(\frac{E_i}{P_i^{-\theta}}\right) \tag{A.21}$$

Inverting the matrices:

$$[X_{ij}]^{-1} = \text{diag}\left(E_i^{-1}\right)\left(\text{diag}\left(P_i^{-\theta}\right)\text{diag}\left(\Pi_i^{-\theta}\right)\text{diag}\left(p_i^{\theta}\right) - [\Xi_{ij}]\right)\text{diag}\left(Y_i^{-1}\right) \tag{A.22}$$

And inverting again:

$$[X_{ij}] = \text{diag}\left(Y_i\right)\left(\text{diag}\left(P_i^{-\theta}\right)\text{diag}\left(\Pi_i^{-\theta}\right)\text{diag}\left(p_i^{\theta}\right) - [\Xi_{ij}]\right)^{-1}\text{diag}\left(E_i\right) \tag{A.23}$$

The objective is now to express $\text{diag}\left(\Pi_i^{-\theta}\right)\text{diag}\left(p_i^{\theta}\right)$ as a function of observables only.

Starting from the definition $P_i^{-\theta} = \sum_j \tau_{ji}^{-\theta}\frac{Y_j}{\Pi_j^{-\theta}}$ and switching to matrix notations – where where $[x_i]$ denotes a $N \times 1$ column matrix of general term x_i:

$$\left[P_i^{-\theta}\right] = \left[\tau_{ij}^{-\theta}\right]'\left[\frac{Y_i}{\Pi_i^{-\theta}}\right] \tag{A.24}$$

$$\left[P_i^{-\theta}\right] = \left(\mathbf{I} - \mathbf{D}'\right)^{-1}\left[p_i^{-\theta}\frac{Y_i}{\Pi_i^{-\theta}}\right] \tag{A.25}$$

$$\left(\mathbf{I} - \text{diag}\left(p_i^{-\theta}\right)\text{diag}\left(\Pi_i^{\theta}\right)[\Xi_{ij}]'\,\text{diag}\left(P_i^{\theta}\right)\right)\left[P_i^{-\theta}\right] = \left[p_i^{-\theta}\frac{Y_i}{\Pi_i^{-\theta}}\right] \tag{A.26}$$

$$\left[\Pi_i^{-\theta}P_i^{-\theta}p_i^{\theta}\right] = [Y_i] + [\Xi_{ij}]'\,[1] \tag{A.27}$$

where $[1]$ is a $N \times 1$ column matrix in which all coefficients are equal to 1.

Similarly, starting from the definition $\Pi_i^{-\theta} = \sum_j \tau_{ij}^{-\theta}\frac{E_j}{P_j^{-\theta}}$ and switching to matrix notations:

$$\left[\Pi_i^{-\theta}\right] = \left[\tau_{ij}^{-\theta}\right]\left[\frac{E_i}{P_i^{-\theta}}\right] \tag{A.28}$$

$$\left[\Pi_i^{-\theta}\right] = (\mathbf{I} - \mathbf{G})^{-1} \left[p_i^{-\theta} \frac{E_i}{P_i^{-\theta}}\right] \tag{A.29}$$

with

$$\mathbf{G} = [g_{ij}] = \text{diag}\left(p_i^{-\theta}\right) \left[\tau_{ij}^{-\theta}\right]$$

$$\left(\mathbf{I} - \text{diag}\left(p_i^{-\theta}\right) \text{diag}\left(P_i^{\theta}\right) [\Xi_{ij}] \, \text{diag}\left(\Pi_i^{\theta}\right)\right) \left[\Pi_i^{-\theta}\right] = \left[p_i^{-\theta} \frac{E_i}{P_i^{-\theta}}\right] \tag{A.30}$$

$$\left[\Pi_i^{-\theta} P_i^{-\theta} p_i^{\theta}\right] = [E_i] + [\Xi_{ij}] \, [1] \tag{A.31}$$

where $[1]$ is a $N \times 1$ column matrix in which all coefficients are equal to 1.

Following A&A, I average the two definitions of $\text{diag}\left(\Pi_i^{-\theta}\right) \text{diag}\left(p_i^{\theta}\right)$:

$$\left[\Pi_i^{-\theta} P_i^{-\theta} p_i^{\theta}\right] = \frac{1}{2} [Y_i + E_i] + \frac{1}{2} \left([\Xi_{ij}]' \, [1] + [\Xi_{ij}] \, [1]\right) \tag{A.32}$$

Finally, plugging into the expression of $[X_{ij}]$ in equation A.23:

$$[X_{ij}] = \text{diag}\left(Y_i\right) \left(\text{diag}\left(\frac{1}{2} [Y_i + E_i] + \frac{1}{2} \left([\Xi_{ij}]' \, [1] + [\Xi_{ij}] \, [1]\right)\right) - [\Xi_{ij}]\right)^{-1} \text{diag}\left(E_i\right) \tag{A.33}$$

i.e., back to vectors notations:

$$X_{ij} = Y_i \left(\mathbf{D}^{\mathbf{X}} - [\Xi_{ij}]\right)^{-1}_{ij} E_j \tag{A.34}$$

where $\mathbf{D}^{\mathbf{X}} = \text{diag}\left(\frac{1}{2} [Y_i + E_i] + \frac{1}{2} \left([\Xi_{ij}]' \, [1] + [\Xi_{ij}] \, [1]\right)\right)$

A.5 Equilibrium with traffic

The first step consists in integrating the analytical relationship between τ_{ij} and t_{ij}, p_i into the equilibrium equations 13 and 14. Starting from the first equilibrium equation 13 and using expression A.7 yields:

$$\bar{A}_i^{-\theta} \bar{l}_i^{-\theta} y_i^{1+\theta} = \sum_j c_{ij}^G p_j^{-\theta} (1 + \kappa_j) y_j P_j^{\theta} \tag{A.35}$$

Switching to matrix notations:

$$\left[\bar{A}_i^{-\theta} \bar{l}_i^{-\theta} y_i^{1+\theta}\right] = \mathbf{C}^{\mathbf{G}} \left[p_i^{-\theta} (1 + \kappa_i) y_i P_i^{\theta}\right] \tag{A.36}$$

where $\left[\bar{A}_i^{-\theta} \bar{l}_i^{-\theta} y_i^{1+\theta}\right]$ and $\left[p_i^{-\theta} (1 + \kappa_i) y_i P_i^{\theta}\right]$ are $N \times 1$ column matrices and $\mathbf{C}^{\mathbf{G}}$ is a $N \times N$

square matrix. Remember that $\mathbf{C^G} = (\mathbf{I} - \mathbf{G})^{-1}$ from A.7, which yields:

$$(\mathbf{I} - \mathbf{G}) \left[\bar{A}_i^{-\theta} \bar{l}_i^{-\theta} y_i^{1+\theta} \right] = \left[p_i^{-\theta} (1 + \kappa_i) y_i P_i^{\theta} \right] \tag{A.37}$$

or in non-matrix notations:

$$\bar{A}_i^{-\theta} \bar{l}_i^{-\theta} y_i^{1+\theta} = p_i^{-\theta} (1 + \kappa_i) y_i P_i^{\theta} + \sum_j p_i^{-\theta} t_{ij}^{-\theta} \bar{A}_j \bar{l}_j^{-\theta} y_j^{\theta+1} \tag{A.38}$$

Similarly with the second equilibrium equation 14 and using expression A.8:

$$P_i^{-\theta} = \sum_j c_{ji}^{D} p_j^{-\theta} \bar{A}_j^{\theta} \bar{l}_j^{\theta} y_j^{-(\theta+1)} \tag{A.39}$$

Switching to matrix notations:

$$\left[P_i^{-\theta} \right] = \left[p_i^{-\theta} \bar{A}_i^{\theta} \bar{l}_i^{\theta} y_i^{-(\theta+1)} \right] \mathbf{C^{D'}} \tag{A.40}$$

where $\left[P_i^{-\theta} \right]$ and $\left[p_i^{-\theta} \bar{A}_i^{\theta} \bar{l}_i^{\theta} y_i^{-(\theta+1)} \right]$ are $N \times 1$ column matrices and $\mathbf{C^D}$ is a $N \times N$ square matrix. Remember that $\mathbf{C^D} = (\mathbf{I} - \mathbf{D})^{-1}$ from A.7, hence $\mathbf{C^{D'}} = (\mathbf{I} - \mathbf{D'})^{-1}$, which yields:

$$\left[P_i^{-\theta} \right] (\mathbf{I} - \mathbf{D'}) = \left[p_i^{-\theta} \bar{A}_i^{\theta} \bar{l}_i^{\theta} y_i^{-(\theta+1)} \right] \tag{A.41}$$

or in non-matrix notations:

$$P_i^{-\theta} = p_i^{-\theta} \bar{A}_i^{\theta} \bar{l}_i^{\theta} y_i^{-(\theta+1)} + \sum_j p_i^{-\theta} t_{ji}^{-\theta} P_j^{-\theta} \tag{A.42}$$

The second step consists in introducing the traffic congestion into equations A.38 and A.42. Combining equation 28 with expression A.1 yields

$$p_i = \bar{\Gamma}_i^{\frac{1}{1-\lambda\theta}} \, e^{\frac{\mu_i}{1-\lambda\theta} \text{ weather}_i} \, \bar{L}^{\frac{\lambda}{1-\lambda\theta}} \bar{A}_i^{\frac{-\lambda\theta}{1-\lambda\theta}} \bar{l}_i^{\frac{-\lambda\theta}{1-\lambda\theta}} P_i^{\frac{-\lambda\theta}{1-\lambda\theta}} \, y_i^{\frac{\lambda(\theta+1)}{1-\lambda\theta}} \tag{A.43}$$

Using this expression to replace p_i in equations A.38 and A.42 leads to the two equilibrium conditions with traffic:

$$\begin{aligned} y_i^{\theta+1+\frac{\lambda\theta(\theta+1)}{1-\lambda\theta}} P_i^{-\frac{\lambda\theta^2}{1-\lambda\theta}} =& \bar{L}^{-\frac{\lambda\theta}{1-\lambda\theta}} \bar{A}_i^{\frac{\lambda\theta^2}{1-\lambda\theta}+\theta} \bar{\Gamma}_i^{\frac{-\theta}{1-\lambda\theta}} e^{\frac{-\mu_i\theta}{1-\lambda\theta}\text{weather}_i} \bar{l}_i^{\frac{\lambda\theta^2}{1-\lambda\theta}+\theta} (1 + \kappa_i) y_i P_i^{\theta} \\ &+ \bar{L}^{-\frac{\lambda\theta}{1-\lambda\theta}} \sum_{j=1}^{N} \bar{A}_i^{\frac{\lambda\theta^2}{1-\lambda\theta}+\theta} \bar{A}_j \bar{t}_{ij}^{-\theta} \bar{\Gamma}_i^{\frac{-\theta}{1-\lambda\theta}} e^{\frac{-\mu_i\theta}{1-\lambda\theta}\text{weather}_i} \bar{l}_i^{\frac{\lambda\theta^2}{1-\lambda\theta}+\theta} \bar{l}_j^{-\theta} y_j^{1+\theta} \end{aligned} \tag{A.44}$$

$$
\begin{aligned}
y_i^{\frac{\lambda\theta(\theta+1)}{1-\lambda\theta}} P_i^{-\theta-\frac{\lambda\theta^2}{1-\lambda\theta}} =& \bar{L}^{\frac{-\lambda\theta}{1-\lambda\theta}} \bar{A}_i^{\frac{\lambda\theta^2}{1-\lambda\theta}+\theta} \bar{\Gamma}_i^{\frac{-\theta}{1-\lambda\theta}} e^{\frac{-\mu_i\theta}{1-\lambda\theta}\text{weather}_i} \bar{l}_i^{\frac{\lambda\theta^2}{1-\lambda\theta}+\theta} y_i^{-\theta+1} \\
&+ \bar{L}^{-\frac{\lambda\theta}{1-\lambda\theta}} \sum_{j=1}^{N} \bar{A}_i^{\frac{\lambda\theta^2}{1-\lambda\theta}} \bar{t}_{ij}^{-\theta} \bar{\Gamma}_i^{\frac{-\theta}{1-\lambda\theta}} e^{\frac{-\mu_i\theta}{1-\lambda\theta}\text{weather}_i} \bar{l}_i^{\frac{\lambda\theta^2}{1-\lambda\theta}} P_j^{-\theta}
\end{aligned} \tag{A.45}
$$

A.6 Exact hat algebra

Consider a counterfactual weather $\{\text{weather}'_i\}_{i\in\mathcal{N}}$ and counterfactual trade deficits $\{(1+\kappa'_i)\}_{i\in\mathcal{N}}$. Combining the market clearing condition $Y_i = \sum_j X_{ij}$ from 9 with equation 10 yields

$$
\Pi_i^{-\theta} = \sum_j \tau_{ij}^{-\theta} E_j P_j^{\theta} \tag{A.46}
$$

Using equation A.8 and switching to matrix notations, it comes:

$$
\left[\Pi_i^{-\theta}\right] = \left(\mathbf{I} - \left[p_i^{-\theta} t_{ij}^{-\theta}\right]\right)^{-1} \left[p_i^{-\theta} E_i P_i^{\theta}\right] \tag{A.47}
$$

where $\left[\Pi_i^{-\theta}\right]$ and $\left[p_i^{-\theta} E_i P_i^{\theta}\right]$ are $N \times 1$ column matrices and $\left[p_i^{-\theta} t_{ij}^{-\theta}\right]$ is a $N \times N$ square matrix. This can be rewritten as

$$
\Pi_i^{-\theta} = p_i^{-\theta} E_i P_i^{\theta} + \sum_j p_i^{-\theta} t_{ij}^{-\theta} \Pi_j^{-\theta} \tag{A.48}
$$

Similarly, combining the market clearing condition $E_j = \sum_i X_{ij}$ from 9 with equation 10 yields

$$
P_j^{-\theta} = \sum_j \tau_{ij}^{-\theta} Y_i \Pi_i^{\theta} \tag{A.49}
$$

Using equation A.7 and switching to matrix notations, it comes:

$$
\left[P_i^{-\theta}\right]' = \left[p_i^{-\theta} Y_i \Pi_i^{\theta}\right]' \left(\mathbf{I} - \left[p_j^{-\theta} t_{ij}^{-\theta}\right]\right)^{-1} \tag{A.50}
$$

which can be rewritten as

$$
P_j^{-\theta} = p_j^{-\theta} Y_j \Pi_j^{\theta} + \sum_i p_j^{-\theta} t_{ij}^{-\theta} P_i^{-\theta} \tag{A.51}
$$

In the counterfactual scenario, equation A.48 will be:

$$
\Pi_i'^{-\theta} = p_i'^{-\theta} E_i' P_i'^{\theta} + \sum_j p_i'^{-\theta} \bar{t}_{ij}^{-\theta} \Pi_j'^{-\theta} \tag{A.52}
$$

where x' denote the counterfactual value of variable x. $\bar{t}_{ij}$ stays the same in the counterfactual world as it is exogenously given, hence not affected by a change in weather. Using the notation $\hat{x}_i \equiv \frac{x'_i}{x_i}$:

$$
\hat{\Pi}_i'^{-\theta} = \frac{1}{\Pi_i^{-\theta}} p_i^{-\theta} E_i P_i^{\theta} \hat{p}_i^{-\theta} \hat{E}_i \hat{P}_i^{\theta} + \sum_j \frac{1}{\Pi_i^{-\theta}} p_i^{-\theta} \bar{t}_{ij}^{-\theta} \Pi_j^{-\theta} \hat{p}_i^{-\theta} \hat{\Pi}_j^{-\theta} \tag{A.53}
$$

Using A.48 to replace $\Pi_i^{-\theta}$ and simplifying yields:

$$\hat{\Pi}_i'^{-\theta} = \frac{E_i}{E_i + \sum_j \bar{t}_{ij} P_i^{-\theta} \Pi_j^{-\theta}} \hat{p}_i^{-\theta} \hat{E}_i \hat{P}_i^{\theta} + \sum_j \left(\frac{\bar{t}_{ij} P_i^{-\theta} \Pi_j^{-\theta}}{E_i + \sum_j \bar{t}_{ij} P_i^{-\theta} \Pi_j^{-\theta}} \right) \hat{p}_i^{-\theta} \hat{\Pi}_j^{-\theta} \tag{A.54}$$

Remember that $\Xi_{ij} = \bar{t}_{ij} P_i^{-\theta} \Pi_j^{-\theta}$ (equation 21). Hence:

$$\hat{\Pi}_i^{-\theta} = \frac{E_i}{E_i + \sum_j \Xi_{ij}} \hat{p}_i^{-\theta} \hat{E}_i \hat{P}_i^{\theta} + \sum_j \left(\frac{\Xi_{ij}}{E_i + \sum_j \Xi_{ij}} \right) \hat{p}_i^{-\theta} \hat{\Pi}_j^{-\theta} \tag{A.55}$$

Similarly, equation A.51 will be in the counterfactual world:

$$P_j'^{-\theta} = p_j'^{-\theta} Y_j' \Pi_j'^{\theta} + \sum_i p_j'^{-\theta} \bar{t}_{ij}^{-\theta} P_i'^{-\theta} \tag{A.56}$$

which can be rewritten as:

$$\hat{P}_j^{-\theta} = \frac{1}{P_j^{-\theta}} \frac{p_j^{-\theta} Y_j}{\Pi_j^{-\theta}} \frac{\hat{p}_j^{-\theta} \hat{Y}_j}{\hat{\Pi}_j^{-\theta}} + \sum_i \frac{p_j^{-\theta} \bar{t}_{ij}^{-\theta} P_i^{-\theta}}{P_j^{-\theta}} \hat{p}_j^{-\theta} \hat{P}_i^{-\theta} \tag{A.57}$$

Using A.51 to replace $P_j^{-\theta}$ and the expression of Ξ_{ij} from equation 21 yields:

$$\hat{P}_j^{-\theta} = \frac{Y_j}{Y_j + \sum_i \Xi_{ij}} \frac{\hat{p}_j^{-\theta} \hat{Y}_j}{\hat{\Pi}_j^{-\theta}} + \sum_i \left(\frac{\Xi_{ij}}{Y_j + \sum_i \Xi_{ij}} \right) \hat{p}_j^{-\theta} \hat{P}_i^{-\theta} \tag{A.58}$$

From equation 28, we can write:

$$\hat{p}_i = e^{\frac{\mu_i}{1-\lambda\theta} \Delta \text{ weather}_i} \hat{P}_i^{\frac{-\lambda\theta}{1-\lambda\theta}} \hat{\Pi}_i^{\frac{-\lambda\theta}{1-\lambda\theta}} \tag{A.59}$$

Plugging this expression in equations A.55 and A.58 leads to:

$$\hat{\Pi}_i^{-\frac{\theta}{1-\lambda\theta}} \hat{P}_i^{-\frac{\theta}{1-\lambda\theta}} = \frac{E_i}{E_i + \sum_j \Xi_{ij}} \hat{E}_i \, e^{\frac{-\mu_i \theta}{1-\lambda\theta} \Delta \text{ weather}_i} + \sum_j \left(\frac{\Xi_{ij}}{E_i + \sum_j \Xi_{ij}} \right) e^{\frac{-\mu_i \theta}{1-\lambda\theta} \Delta \text{ weather}_i} \hat{P}_i^{-\theta} \hat{\Pi}_j^{-\theta} \tag{A.60}$$

$$\hat{P}_i^{-\frac{\theta}{1-\lambda\theta}} \hat{\Pi}_i^{-\frac{\theta}{1-\lambda\theta}} = \frac{Y_i}{Y_i + \sum_j \Xi_{ji}} \hat{Y}_i \, e^{\frac{-\mu_i \theta}{1-\lambda\theta} \Delta \text{ weather}_i} + \sum_j \left(\frac{\Xi_{ji}}{Y_i + \sum_j \Xi_{ji}} \right) e^{\frac{-\mu_i \theta}{1-\lambda\theta} \Delta \text{ weather}_i} \hat{P}_j^{-\theta} \hat{\Pi}_i^{-\theta} \tag{A.61}$$

Finally, from equation A.1 I get

$$\hat{\Pi}_i = \hat{y}_i^{-\frac{\theta+1}{\theta}} \tag{A.62}$$

and from equation 12 it comes

$$\hat{E}_i = \widehat{(1+\kappa_i)}\hat{y}_i \tag{A.63}$$

Plugging these two expressions into equations A.60 and A.61 yields the two exact hat equilibrium equations 31 and 32:

$$\begin{aligned}\hat{y}_i^{\frac{1+\theta}{1-\lambda\theta}}\hat{P}_i^{\frac{-\theta}{1-\lambda\theta}+\theta} = &\left(\frac{E_i}{E_i+\sum_j \Xi_{ij}}\right) e^{\frac{-\mu_i\theta}{1-\lambda\theta}\Delta\text{weather}_i}\widehat{(1+\kappa_i)}\hat{y}_i\hat{P}_i^{\theta} \\ &+\sum_{j=1}^{N}\left(\frac{\Xi_{ij}}{E_i+\sum_j \Xi_{ij}}\right) e^{\frac{-\mu_i\theta}{1-\lambda\theta}\Delta\text{weather}_i}\hat{y}_j^{\theta+1}\end{aligned} \tag{A.64}$$

$$\begin{aligned}\hat{y}_i^{\frac{\theta+1}{1-\lambda\theta}-(\theta+1)}\hat{P}_i^{\frac{-\theta}{1-\lambda\theta}} = &\left(\frac{Y_i}{Y_i+\sum_j \Xi_{ji}}\right) e^{\frac{-\mu_i\theta}{1-\lambda\theta}\Delta\text{weather}_i}\hat{y}_i^{-\theta} \\ &+\sum_{j=1}^{N}\left(\frac{\Xi_{ji}}{Y_i+\sum_j \Xi_{ji}}\right) e^{\frac{-\mu_i\theta}{1-\lambda\theta}\Delta\text{weather}_i}\hat{P}_j^{-\theta}\end{aligned} \tag{A.65}$$

B Further reduced-form evidence

B.1 Other weather variables

Table B.1: Effect of monthly average weather on port average dwell time

	(1)	(2)	(3)	(4)
water level	0.0502*			
	(0.0296)			
wave height		0.0238***		
		(0.0066)		
wind speed			0.0148***	
			(0.0056)	
precipitations				0.0103***
				(0.0033)
# observations	92,434	92,434	92,434	92,434
# ports	1,675	1,675	1,675	1,675

NB: standardized coefficients, describing the effect of a +1 st.dev.
Standard errors (clustered by port) in parentheses
* $p < 0.10$, ** $p < 0.05$, *** $p < 0.01$

B.2 Effect on traffic

$$\ln(\text{traffic})_{it} = \alpha + \beta \ \text{waterlevel}_{it} + \delta_i + \delta_t + \epsilon_{it} \tag{B.66}$$

Table B.2: Effect of water level on port entering traffic

	(1)	(2)	(3)	(4)	(5)
	t = day	t = week	t = month	t = quarter	t = year
water level in i	-0.0085***	-0.0039	0.0051	-0.0043	-0.8240**
	(0.0027)	(0.0067)	(0.0283)	(0.0524)	(0.3936)
# observations	2,012,170	525,374	147,041	49,482	12,946
# ports	1,679	1,679	1,679	1,679	1,678

Standard errors (clustered by port) in parentheses
* $p < 0.10$, ** $p < 0.05$, *** $p < 0.01$

B.3 Non-linear specifications

Table B.3: Effect of water level bins on port average dwell time

	(1) t = day	(2) t = week	(3) t = month	(4) t = quarter
water level $\in [0, 0.65\text{m})$	*ref*	*ref*	*ref*	*ref*
water level $\in [0.65, 1.95\text{m})$	0.0166***	0.0302***	0.0668**	0.1218**
	(0.0032)	(0.0086)	(0.0305)	(0.0537)
water level $\in [1.95, 3.90\text{m})$	0.0249***	0.0403**	0.1011	0.0290
	(0.0057)	(0.0164)	(0.0683)	(0.1290)
water level $\in [3.90, +\infty\text{m})$	0.0434***	0.0930***	0.2872**	0.3414
	(0.0117)	(0.0291)	(0.1188)	(0.2295)
# observations	1,994,540	520,533	146,081	53,183
# ports	1,679	1,679	1,679	1,679

Standard errors (clustered by port) in parentheses

* $p < 0.10$, ** $p < 0.05$, *** $p < 0.01$

Table B.4: Effect of water level relative bins on port average dwell time

	(1) t = day	(2) t = week	(3) t = month
water level $\in [0, p50\text{m})$	*ref*	*ref*	*ref*
water level $\in [p50, p90\text{m})$	0.0073***	0.0101*	0.0034
	(0.0019)	(0.0055)	(0.0172)
water level $\in [p90, p99\text{m})$	0.0224***	0.0419***	0.0336
	(0.0036)	(0.0086)	(0.0239)
water level $\in [p99, +\infty\text{m})$	0.0378***	0.0865***	0.1055
	(0.0077)	(0.0218)	(0.0681)
# observations	1,994,540	520,533	146,081
# ports	1,679	1,679	1,679

Standard errors (clustered by port) in parentheses

* $p < 0.10$, ** $p < 0.05$, *** $p < 0.01$

B.4 Daily event-studies

To decompose the effect of weather shocks and the potential leads and lags effects, I consider an event-study setting at the day level. I consider the effect of a binary treatment $\mathbb{1}\{\text{weather}_{it} > p99\text{weather}_i\}$ on the days before / after it happens, using an event study setting.[27] I rely on the local projection difference-in-differences (LP-DiD) setting of (Dube et al., 2023), to allow to non-absorbing treatment and potential multiple treatments:

$$y_{i,t+h} - y_{i,t-1} = \beta_h \Delta D_{it} + \delta_t^h + \delta_{im}^h + \epsilon_{it}^h \tag{B.67}$$

where D_{it} is the (binary) treatment status of port i on day t and Δ denotes first-difference operator, with sample restriction:

$$\begin{cases} \text{treatment:} & D_{i,t+j} = 1 \text{ for } 0 \leq j \leq h, \qquad D_{i,t-j} = 0 \text{ for } 1 \leq j \leq L \\ \text{clean control:} & D_{i,t-j} = 0 \text{ for } -h \leq j \leq L \end{cases} \tag{B.68}$$

where L is the number of periods after which the dynamic effects stabilize. I keep in the sample only clean treatment (ports that remain in treatment for the post-event window and that have not experienced a treatment close before the one we are considering) and clean controls (ports are not close to a treatment, either before or after). I also control for potential non-parallel trends with port-month fixed effects. To account for the fact that this setting assumes no anticipation and that the clean treated and control conditions assume no change of treatment status (i.e. no entry into treatment and no exit of treatment), I define treatment as 12 days around the extreme event (2 days before, 10 days after).

Figure B.1 and B.2 show the results with weather measured respectively as water level and wave height. For dwell time, the effect the shock is bigger one day before the event, but does not seem to last after. The number of port calls is reduced both before and after, but there seems to be a slight catch up afterwards for high waves – but which does not compensate the negative effect.

[27] With this definition of event, I am potentially comparing days where the weather is above the 99th percentile, to days where it is slightly below: this would tend to attenuate the results.

Figure B.1: Event study results: effect extreme water level on daily port efficiency

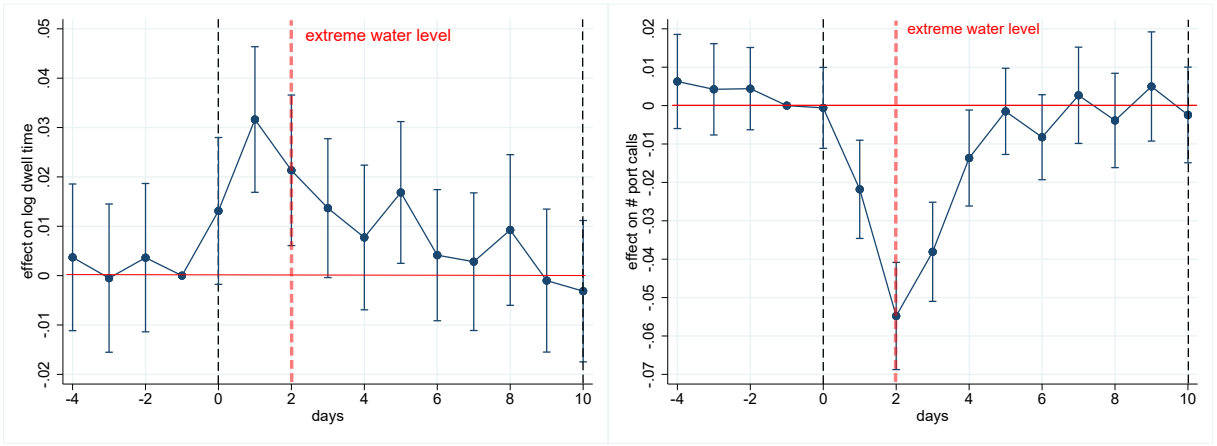

(a) Dwell time (b) Number of entering calls

Figure B.2: Event study results: effect extreme wave height on daily port efficiency

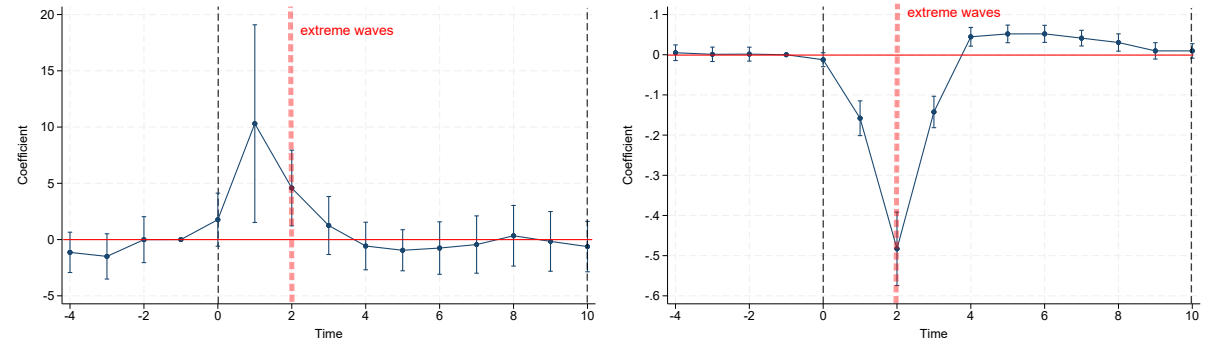

(a) Dwell time (b) Number of entering calls

B.5 Reduced-form at the ship level

The data allow to estimate the effect of weather shocks on ships dwell time at the ship level (without aggregating to port averages):

$$\ln(\text{time}_{sit}) = \beta \text{ weather}_{it} + \delta_{si} + \delta_t + \delta_{iy} + \epsilon_{sit} \tag{B.69}$$

where s denotes a ship, i a port, t a day and y a year. time_{sit} is the dwell time experienced by ship s in port i on day t. weather_{it} is the weather at port i during day t – measured either by average daily wave height or by non-linear bins of wave height.

The results in the table below show effects similar to the ones found at the port level: higher water level increases ship dwell time, an effect which is mostly driven by extreme events.

Table B.5: Effect of total water level on ship dwell time, at the ship level

log dwell time	(1)	(2)	(3)
water level	0.0203***		
	(0.0025)		
water level >2m		0.0068***	
		(0.0018)	
water level >p95			0.0213***
			(0.0023)
date (day) FE	✓	✓	✓
ship-port FE	✓	✓	✓
port-year FE	✓	✓	✓
SE cluster level	ship, port	ship, port	ship, port
# observations	6,875,918	6,875,918	6,875,918
# clusters	1,676	1,676	1,676

Standard errors in parentheses

* $p < 0.10$, ** $p < 0.05$, *** $p < 0.01$

B.6 Effects outside of the port

When a port is disrupted, ships might prefer to wait outside of the port, to avoid paying additional port fees. This mechanism is not captured in the baseline specification as port calls data only allow to observe when ships actually enter inside the port. However, I can look at the effect of weather shocks in origin or departure port, on the duration of ships trips – i.e. the amount of time between the moment they leave their origin port and the moment they arrive at their destination port. If ships tend to wait outside of ports when there is bad weather, this should increase their trip time.

I consider the following specification:

$$log(\text{trip time})_{sod,t} = \beta_o \text{ weather}_{o,t} + \beta_d \text{ weather}_{d,t+\text{trip time}} + \delta_s + \delta_{od} + \delta_t + \epsilon_{sod,t} \quad \text{(B.70)}$$

where $\text{trip time}_{sod,t}$ is the trip time of ship s going from origin port o to destination port d on day t (day of departure), $\text{weather}_{o,t}$ is the weather in port of origin at the day of departure, $\text{weather}_{d,t+\text{trip time}}$ the weather in port of destination at the day of arrival. I consider different sets of fixed effects: day, route, ship, ship-route, route-year.

Table B.6 shows the results measuring weather as wave height. These results seem constant over the different sets of fixed effects. They confirm the hypothesized mechanism: +1m in wave height at the origin port increases trip duration by 1.3%, while +1m in wave height at the destination port increases trip duration by 2.2%. In column (4), I remove the shortest

routes (trimming at the top and bottom 25%) to make sure that the weather along the route is not correlated with weather in the ports of departure and arrival, and still find a positive and significant effect.

Table B.6: Effect of origin and destination ports wave height on ships trip duration

	(1)	(2)	(3)	(4)
wave height at origin port	0.0139***	0.0133***	0.0135***	0.0159***
	(0.0011)	(0.0012)	(0.0012)	(0.0015)
wave height at destination port	0.0222***	0.0224***	0.0224***	0.0279***
	(0.0011)	(0.0012)	(0.0012)	(0.0016)
date (day) FE	✓	✓	✓	✓
route (o-d) FE	✓			
ship FE	✓			
ship-route FE		✓	✓	✓
route-year FE			✓	✓
route distance restriction				✓
# observations	5,770,534	5,289,930	5,278,881	2,652,050
# routes	14,109	14,101	14,054	7,137

Standard errors in parentheses

* $p < 0.10$, ** $p < 0.05$, *** $p < 0.01$

This means the effects measured *inside* the ports might be only a lower bound of the full effects, since they do not capture ships waiting *outside* of ports.

B.7 Routes vs Ports

Delays in shipping can also happen because of weather conditions along the maritime route, i.e. in the journey between two ports. I compare the effects on shipping of weather along the maritime route and weather in the port, using the following specification:

$$\text{time}_{sit} = \beta \text{ weather}_{it} + \delta_{si} + \delta_t + \delta_{im} + \delta_{iy} + \epsilon_{sit} \tag{B.71}$$

where s is a ship, i either a *route* or a *port*, and t a day. time_{sit} denotes the time (in hours) spent by ship s along the route i or in the port i[28], $weather_{it}$ denotes the weather conditions (wave height) along the route i or in the port i – measured either as average daily wave height or bins of daily wave height. I also include ship-port (resp. ship-route) fixed effects, date fixed effects, port-month-of-the-year (resp. route-month-of-the-year) fixed effects, and port-year (resp. route-year) fixed effects.

[28]To ensure a better comparability between ports and routes, the dependent variable is in levels rather than in log, to quantify the effect in terms of additional hours of shipping.

To measure shipping time and weather along the maritime routes, I focus on trips happening on the 300 most frequent routes present in the shipping data. I compute trip duration as the difference between the time of destination port arrival and origin port departure. Since I only observe the origin and destination ports and not the exact trajectory of the ship in between, I rely on SeaRoute algorithm to compute the shortest route by sea between these two ports. Using gridded wave height from ERA5, I compute the weather along a route for a given day as a weighted average of the grid points weather, where the weights are the inverse of distance between the grid point and the route, times a measure of the density of grid cells at the point location.

The results in Table B.7 show that the effect on weather along the route or in the port tend to be pretty similar: an increase of 1m of average wave height along the route or at the port increases shipping time by 0.7 hour. Port extreme weather events seems to have a slightly more important effect than route extreme weather events: a wave height greater than 2m at the port adds 1.5 hour of shipping time compared to a wave height lower than 0.5m, again 1.2 additional hour for a wave height greater than 2m at along the route.

Weather at port hence seems to be only marginally more important than weather at sea. However, weather at port can influence time spent on the route, as highlighted in section B.6, because ships tend to lower their speed (or stop) when their destination port is congested. But weather along the route seems more unlikely to influence the time spent at ports. To test these mechanisms, I consider a similar specification:

$$\text{time}_{sit} = \beta \ \text{weather}_{jt} + \delta_{si} + \delta_t + \delta_{im} + \delta_{iy} + \epsilon_{sit} \tag{B.72}$$

where either i is a route, in which case j is the destination port of this route – i.e. I measure the effect of weather in the destination port on the time spend on the route (expected to be positive, as in section B.6); or i is a port, in which case j is a route arriving at port i – i.e. I investigate the effect of weather along a route on the time spent in destination port (expected to be close to null).

The results in Table B.8 show that indeed, port weather can have a significant effect on time spent along the route (columns 1 and 2), but the reverse is not true (columns 3 and 4). Hence adverse weather conditions in a port increase significantly the shipping time, both because of higher time spent in the port and along the route ; while time at sea has a smaller effect, only along the route. This justifies focusing on the effects of weather in the ports.

B.8 Traffic diversion within the network

Table B.7: Direct effect of weather on shipping time – comparison between routes and ports

	route weather on route time		port weather on port time	
	(1)	(2)	(3)	(4)
average wave	0.6791***		0.6795***	
	(0.0773)		(0.1198)	
wave <0.5m		*ref*		*ref*
wave 0.5-0.8m		0.0597		0.0894
		(0.0419)		(0.1000)
wave 0.8-1.3m		0.1472**		0.3137**
		(0.0601)		(0.1432)
wave 1.3-2m		0.4616***		0.5767***
		(0.0986)		(0.2009)
wave >2m		1.2374***		1.4580***
		(0.1480)		(0.2454)
unit	route	route	port	port
date (day) FE	✓	✓	✓	✓
ship-unit FE	✓	✓	✓	✓
unit-month FE	✓	✓	✓	✓
unit-year FE	✓	✓	✓	✓
# observations	1,555,030	1,555,030	6,905,453	6,905,453
# clusters	255	255	1,664	1,664

Standard errors in parentheses

* $p < 0.10$, ** $p < 0.05$, *** $p < 0.01$

Table B.8: Cross effect of weather on shipping time – comparison between routes and ports

	port weather on route time		route weather on port time	
	(1)	(2)	(3)	(4)
average wave	0.9510***		0.0863	
	(0.0489)		(0.0794)	
wave <0.5m		*ref*		*ref*
wave 0.5-0.8m		0.2030***		-0.2766**
		(0.0314)		(0.1207)
wave 0.8-1.3m		0.5284***		-0.2444*
		(0.0421)		(0.1457)
wave 1.3-2m		1.0529***		-0.1409
		(0.0636)		(0.1543)
wave >2m		1.8893***		0.2233
		(0.1136)		(0.2036)
weather	port	port	route	route
unit	route	route	port	port
date (day) FE	✓	✓	✓	✓
ship-unit FE	✓	✓	✓	✓
unit-month FE	✓	✓	✓	✓
unit-year FE	✓	✓	✓	✓
# observations	5,265,994	5,265,994	426,331	426,331
# clusters	13,605	13,605	101	101

Standard errors in parentheses

* $p < 0.10$, ** $p < 0.05$, *** $p < 0.01$

Table B.9: Effect of water level in intermediate ports on traffic share along a route

	t = month		t = quarter		t = year	
	(1)	(2)	(3)	(4)	(5)	(6)
water level in int. ports	-1.4668***	-1.1502***	-2.4366***	-1.7811***	-13.0468***	-21.3831**
	(0.1787)	(0.1839)	(0.3537)	(0.3800)	(2.8259)	(8.5305)
route FE	✓	✓	✓	✓	✓	✓
port-pair FE	✓		✓		✓	
port-pair-year FE		✓		✓		✓
date FE	✓	✓	✓	✓	✓	✓
control for port-pair avg weather		✓		✓		✓
control for lag weather		✓		✓		✓
SE cluster level	route	port pair	route	port pair	route	port pair
# observations	1,847,662	1,847,662	793,361	793,361	152,423	152,423
# clusters	234,290	39,191	157,669	32,626	51,362	11,493

Standard errors in parentheses

* $p < 0.10$, ** $p < 0.05$, *** $p < 0.01$

C Additional estimation results

Table C.10: Effect of moving traffic and water level on port dwell time, accounting for climate heterogeneity

	(1)	(2) OLS	(3) IV
water level (MA)	0.04178***	0.02849***	0.01796*
	(0.01035)	(0.00984)	(0.00975)
water level (MA) × period-avg	-0.00622*	-0.00408	-0.00238
	(0.00372)	(0.00336)	(0.00331)
log traffic (MA)		0.13750***	0.24643***
		(0.00637)	(0.03507)
date FE	✓	✓	✓
ship-port FE	✓	✓	✓
port-year FE	✓	✓	✓
# observations	6,123,769	6,123,769	6,123,769
# ships	11,311	11,311	11,311
# ports	1,620	1,620	1,620
First Stage KP-F			156.3

Standard errors in parentheses, two-way clustered at the ship and port levels.
* $p < 0.10$, ** $p < 0.05$, *** $p < 0.01$

D Computing counterfactuals

The international trade setting requires to take into account trade deficit between locations. I follow the trade literature to handle this feature in the empirical application, in two steps.

First, given baseline $\{\Xi_{ij0}, Y_{i0}, E_{i0}\}$ observed in the data, I compute counterfactual outcomes assuming no weather shock ($\Delta\text{weather}_i = 0 \quad \forall i \in \mathcal{N}$), but deficits go to zero ($\kappa_i' = 0$, i.e. $\widehat{(1+\kappa_i)} = \frac{1}{1+\kappa_i} = \frac{Y_i}{E_i} \quad \forall i \in \mathcal{N}$). It amounts to solving the following system of equations:

$$\hat{y}_{i1}^{\frac{1+\theta}{1-\lambda\theta}} \hat{P}_{i1}^{\frac{-\theta}{1-\lambda\theta}+\theta} = \left(\frac{Y_{i0}}{E_{i0} + \sum_j \Xi_{ij0}}\right) \hat{y}_{i1} \hat{P}_{i1}^{\theta} + \sum_{j=1}^{N} \left(\frac{\Xi_{ij0}}{E_{i0} + \sum_j \Xi_{ij0}}\right) \hat{y}_{j1}^{\theta+1} \tag{D.73}$$

$$\hat{y}_{i1}^{\frac{\theta+1}{1-\lambda\theta}-(\theta+1)} \hat{P}_{i1}^{\frac{-\theta}{1-\lambda\theta}} = \left(\frac{Y_{i0}}{Y_{i0} + \sum_j \Xi_{ji0}}\right) \hat{y}_{i1}^{-\theta} + \sum_{j=1}^{N} \left(\frac{\Xi_{ji0}}{Y_{i0} + \sum_j \Xi_{ji0}}\right) \hat{P}_{j1}^{-\theta} \tag{D.74}$$

This allows to retrieve first step counterfactual levels of outcome $Y_{i1} = Y_{i0}\ \hat{y}_{i1}$ and traffic flows $\Xi_{ij1} = \Xi_{ij0}\ \hat{\Xi}_{ij1}$: those are the outcome levels if the weather profile stays the same as in the

baseline period, but the trade gets balanced. By definition, we then have $Y_{i1} = E_{i1}$.

Second, given $\{\Xi_{ij1}, Y_{i1}\}$ resulted form the first step, I compute counterfactual outcomes assuming that the trade deficits stay to zero ($\kappa_i = \kappa_i' = 0$, $\widehat{(1+\kappa_i)} = 1 \quad \forall i \in \mathcal{N}$) but that weather changes ($\{\Delta\text{weather}_i\}_{i\in\mathcal{N}}$). It amounts to solving the following system of equations:

$$\hat{y}_{i2}^{\frac{1+\theta}{1-\lambda\theta}} \hat{P}_{i2}^{\frac{-\theta}{1-\lambda\theta}+\theta} = \left(\frac{Y_{i1}}{E_{i1} + \sum_j \Xi_{ij1}}\right) e^{\frac{-\mu_i\theta}{1-\lambda\theta}\Delta\text{weather}_i} \hat{y}_{i2}\hat{P}_{i2}^{\theta} + \sum_{j=1}^{N} \left(\frac{\Xi_{ij1}}{Y_{i1} + \sum_j \Xi_{ij1}}\right) e^{\frac{-\mu_i\theta}{1-\lambda\theta}\Delta\text{weather}_i} \hat{y}_{j2}^{\theta+1} \tag{D.75}$$

$$\hat{y}_{i2}^{\frac{\theta+1}{1-\lambda\theta}-(\theta+1)} \hat{P}_{i2}^{\frac{-\theta}{1-\lambda\theta}} = \left(\frac{Y_{i1}}{Y_{i1} + \sum_j \Xi_{ji1}}\right) e^{\frac{-\mu_i\theta}{1-\lambda\theta}\Delta\text{weather}_i} \hat{y}_{i2}^{-\theta} + \sum_{j=1}^{N} \left(\frac{\Xi_{ji1}}{Y_{i1} + \sum_j \Xi_{ji1}}\right) e^{\frac{-\mu_i\theta}{1-\lambda\theta}\Delta\text{weather}_i} \hat{P}_{j2}^{-\theta} \tag{D.76}$$

I compute the treatment effect of the change in weather as the difference between equilibrium levels in the two counterfactuals, i.e. nominal outcome changes $\hat{y}_{i2}$ and real outcome changes $\hat{y}_{i2}/\hat{P}_{i2}$.

This method is standard in international trade literature to address deficits (Ossa, 2016). An alternative approach would be to compute just one counterfactual holding the deficits fixed relative to the observed equilibrium; however, this method causes convergence issues.

E Algorithm for conducting counterfactuals

I adapt the algorithm of Allen & Arkolakis (2022) to find the equilibrium in our counterfactual simulations. It consists of a loop solving for vectors of $\{\hat{y}_i\}$ and $\{\hat{P}_i\}$. Equilibrium equations 31 and 32 form a system of non-linear equations in $\{\hat{y}_i\}$ and $\{\hat{P}_i\}$. At the same time, the term on the left-hand side of each of the equilibrium conditions is a log-linear combination of the endogenous variables.

I start with an initial guess of the endogenous variables $\{\hat{y}_i\}_{(0)} = 1$ and $\{\hat{P}_i\}_{(0)} = 1$ and plug it into the equilibrium conditions 31 and 32. To help us update the guess, I define the following:

$$\hat{x}_{1,i} \equiv \hat{y}_i^{\theta+1+\frac{\lambda\theta(\theta+1)}{1-\lambda\theta}} \hat{P}_i^{-\frac{\lambda\theta^2}{1-\lambda\theta}}$$

$$\hat{x}_{2,i} \equiv \hat{y}_i^{\frac{\lambda\theta(\theta+1)}{1-\lambda\theta}} \hat{P}_i^{-\theta-\frac{\lambda\theta^2}{1-\lambda\theta}}$$

so that:

$$\begin{pmatrix} \ln \hat{x}_{1,i} \\ \ln \hat{x}_{2,i} \end{pmatrix} = \begin{pmatrix} \theta + 1 + \frac{\lambda\theta(\theta+1)}{1-\lambda\theta} & -\frac{\lambda\theta^2}{1-\lambda\theta} \\ \frac{\lambda\theta(\theta+1)}{1-\lambda\theta} & -\theta - \frac{\lambda\theta^2}{1-\lambda\theta} \end{pmatrix} \begin{pmatrix} \ln \hat{y}_i \\ \ln \hat{P}_i \end{pmatrix} \iff$$

$$\begin{pmatrix} \ln \hat{y}_i \\ \ln \hat{P}_i \end{pmatrix} = \begin{pmatrix} \theta + 1 + \frac{\lambda\theta(\theta+1)}{1-\lambda\theta} & -\frac{\lambda\theta^2}{1-\lambda\theta} \\ \frac{\lambda\theta(\theta+1)}{1-\lambda\theta} & -\theta - \frac{\lambda\theta^2}{1-\lambda\theta} \end{pmatrix}^{-1} \begin{pmatrix} \ln \hat{x}_{1,i} \\ \ln \hat{x}_{2,i} \end{pmatrix}$$

By this definition, for a guess of $\left(\{\hat{y}_i\}_{(0)}, \{\hat{P}_i\}_{(0)}\right)$, the equilibrium conditions yield a set of vectors $\left(\{\hat{x}_{1,i}\}_{(1)}, \{\hat{x}_{2,i}\}_{(1)}\right)$, which by the log-linear transformation defined above, imply an updated guess of $\left(\{\hat{y}_i\}_{(1)}, \{\hat{P}_i\}_{(1)}\right)$. On each iteration, I rescale the vectors $\left(\{\hat{x}_{1,i}\}_{(1)}, \{\hat{x}_{2,i}\}_{(1)}\right)$ such that the second period income distribution still sums to 1, and update the guess of $\left(\{\hat{y}_i\}_{(0)}, \{\hat{P}_i\}_{(0)}\right)$ towards $\left(\{\hat{x}_{1,i}\}_{(1)}, \{\hat{x}_{2,i}\}_{(1)}\right)$. I iterate through this procedure until the equilibrium conditions are solved. Therefore, this loop returns a $\left(\{\hat{y}_i\}_{(0)}, \{\hat{P}_i\}_{(0)}\right)$ for which:[29]

$$(\hat{x}_{1,i})_{(1)} = \left(\frac{E_i}{E_i + \sum_j \Xi_{ij}}\right) e^{\frac{-\mu_i\theta}{1-\lambda\theta}\Delta\text{weather}_i} (\hat{y}_i)_{(0)} (\hat{P}_i)^{\theta}_{(0)} + \sum_{j=1}^{N} \left(\frac{\Xi_{ij}}{E_i + \sum_j \Xi_{ij}}\right) e^{\frac{-\mu_i\theta}{1-\lambda\theta}\Delta\text{weather}_i} (\hat{y}_j)^{\theta+1}_{(0)}$$

$$(\hat{x}_{2,i})_{(1)} = \left(\frac{Y_i}{Y_i + \sum_j \Xi_{ji}}\right) e^{\frac{-\mu_i\theta}{1-\lambda\theta}\Delta\text{weather}_i} (\hat{y}_i)^{-\theta}_{(0)} + \sum_{j=1}^{N} \left(\frac{\Xi_{ji}}{Y_i + \sum_j \Xi_{ji}}\right) e^{\frac{-\mu_i\theta}{1-\lambda\theta}\Delta\text{weather}_i} (\hat{P}_j)^{-\theta}_{(0)}$$

[29] This system assumes a constant deficit ratio κ; however the system can be adapted straightforwardly to consider rather a change in trade deficit, as done in the first step of Section D.